POLITECNICO DI MILANO

School of Industrial and Information Engineering

Department of Chemistry, Materials and Chemical Engineering

Scuola Giulio Natta

Master Degree in Materials Engineering and Nanotechnology

Plating of Zn-Ni alloy from acidic electrolytes for corrosion protection

Supervisor:
Prof. Luca Magagnin

Assistant supervisor:
Ing. Simona Ieffa

Luigi Sironi

Matr.798712

Academic Year 2015/2016

Abstract (English)

Zinc nickel alloy offers superior corrosion protection to steel as the alloy dissolves more slowly than pure zinc. The degree of protection depends on composition and grain structure of the coating. Bath composition determines plated layer properties, in particular the additives. Hydrogen penetration in substrate during plating is a critical aspect due to consequent embrittlement of steel.

In this work commercial acidic and alkaline baths are used to deposit 10 μm thick layer with a content of nickel from 12% to 16%, common characteristic for corrosion protective coating; in particular we focus on ECOLUX STEEL^{TM}. Effect of deposition parameters (potential, current, stirring) on deposit are studied.

Ciclic voltammetries highlight effects of acidic bath additives. ECOLUX STEEL A works as grain-refining agent, its effect can be observed in SEM image; it affects anodic branch of voltammetries. ECOLUX STEEL C works as complexing agent, it improve deposition in fact current of voltammetry signal increases.

Additives decrease hydrogen penetration, reducing embrittlement effects on steel substrate. GDOES studies on plated fasteners highlight better behaviour of ECOLUX STEEL^{TM} than zinc plating: zinc nickel process removes almost completely hydrogen species into substrate.

Potentiodynamic polarization of plated bolts with different surface finishing shows positive effect of chromium passivation and heat treatment on corrosion resistance: both corrosion current and potential decrease.

Abstract (Italian)

Le leghe zinco nichel offrono miglior una protezione alla corrosione ai substrati d'acciaio rispetto allo zinco puro, perchè si dissolvono più lentamente. Il grado di protezione dipende dalla composizione e dalla struttura cristallina del rivestimento. La composizione del bagno determina le proprietà del film depositato; gli additivi svolgono un ruolo importante in questo. La penetrazione di idrogeno nel substrato durante la deposizione è un aspetto critico, può favorire infatti l'infragilimento dell'acciaio.

In questo lavoro abbiamo usato bagni commerciali acidi e alcalini per depositare un film di 10 µm con un contenuto di nichel tra il 12% e il 16%. Abbiamo analizzato in particolare l'ECOLUX STEEL^{TM}. Abbiamo osservato gli effetti dei parametri di deposizione (potenziale/corrente imposti, agitazione) sul deposito.

La voltammetria ciclica evidenzia gli effetti degli additivi del bagno acido. ECOLUX STEEL A cambia la struttura dei grani come possiamo osservare dall'immagine al SEM; infatti modifica profondamente il ramo anodico della voltammetria. ECOLUX STEEL C è il complessante, favorisce la deposizione della fase ottimale infatti crescono I picchi della voltammetry.

Gli additivi riducono la penetrazione dell'idrogeno, diminuendo l'infragilimento del substrato. Il profilo GDOES di bulloni rivestiti evidenziano il miglior comportamento dell'ECOLUX STEEL^{TM} rispetto alla zincatura: la zinco nichelatura non presenta idrogeno all'interfaccia del substrato.

La potenziodinamica sui bulloni rivestiti mostra l'effetto positive della cromatura e del trattamento termico: diminuisce sia il potenziale sia la corrente di corrosione, quindi assicura una miglior protezione.

Riassunto

Lo zinco è l'elemento più comunemente usato per rivestimenti anticorrosivi su substrati metallici, in particolare l'acciaio. L'elettrodeposizione è il principale processo per la deposizione di questi film, mediante bagni sia acidi che alcalini.

Negli ultimi decenni l'interesse si è concentrato su leghe a base di zinco per assicurare prestazioni sempre migliori in ogni caso specifico. Le leghe zinco nickel si sono dimostrate le più adatte in funzione anticorrosiva; ad oggi risultano la soluzione più usata per rivestire piccoli pezzi metallici, ad esempio la bulloneria. Il nichel rende la lega più nobile del solo zinco, rallentando la corrosione. La dissoluzione preferenziale dello zinco causa la trasformazione della struttura cristallina; i prodotti di corrosione sigillano le cricche causate dallo stress, proteggendo il substrato. L'elettrodeposizione da bagni zinco nichel è di tipo anomalo, con deposizione preferenziale del metallo meno nobile. In base alla composizione della lega si possono ottenere diverse fasi: η, δ, γ e α al crescere del contenuto di nichel. Depositi omogenei di sola fase γ (12-16% Ni) offrono la migliore protezione alla corrosione. I principali fattori che influiscono sulla struttura cristallina sono la composizione del bagno (rapporto Zn^{++}/Ni^{++}, additivi) e i parametri di deposizione (potenziali/correnti imposti, agitazione).

I bagni si possono distinguere in acidi, a base di cloruri o solfati, e alcalini, contenenti idrossidi solitamente di sodio. Gli additivi, principalmente composti organici, possono svolgere diverse funzioni, modificando sostanzialmente il deposito. I complessanti stabilizzano gli ioni in soluzione, controllandone la deposizione. I livellanti e brillantanti sono adsorbiti sulla superficie catodica, regolano il trasferimento degli ioni evitando la formazione di protuberanze e avvallamenti; così si ottiene una superficie più liscia e di conseguenza più brillante. Alcuni additivi sono in grado di controllare la deposizione degli ioni modificando la struttura cristallina e la forma dei grani. Un aspetto critico dell'elettrodeposizione a base di zinco è l'incorporazione di idrogeno e la conseguente diffusione nel substrato con il pericolo di danni per infragilimento.

In questo lavoro abbiamo studiato alcuni bagni commerciali sia acidi che alcalini per deposizione di zinco nichel. In particolare abbiamo concentrato la nostra attenzione

sull'ECOLUX STEEL^{TM}, un prodotto della GLOMAX srl che ringraziamo per la collaborazione, osservando anche come gli additivi influenzino il comportamento del bagno. Abbiamo iniziato con la ricerca dei parametri ottimali per la deposizione di uno film di circa 10 μm con un contenuto di nichel tra il 12% e il 16% su un lamierino d'acciaio. Abbiamo studiato l'effetto dell'agitazione e della variazione del potenziale di deposizione sulla composizione del deposito. Per le soluzioni acide gli additivi assicurano il contenuto ottimale di nichel per un largo intervallo di potenziale. La XRD ci mostra che i depositi ottenuti sono composti quasi unicamente di fase γ.

La voltammetria ciclica permette di studiare l'effetto dei singoli additivi sul comportamento elettrochimico del bagno acido. ECOLUX STEEL A modifica profondamento il ramo anodico e ne sposta i potenziali; questo indica una variazione della struttura cristallina del deposito ad opera di un additivo adsorbito sulla superficie. Possiamo quindi attribuirgli la modifica della morfologia osservata al SEM, con formazione di cristalli più piccoli, allungati e compatti. ECOLUX STEEL C rende i picchi più alti e definiti, è un complessante che favorisce la deposizione della fase desiderata.

Mediante la GDOES osserviamo come gli additivi riescano a ridurre l'idrogeno all'interfaccia del substrato. I profili GDOES dei bulloni confermano questo risultato: mentre dopo una semplice zincatura abbiamo idrogeno all'interno del substrato, con la zinco nichelatura il segnale si annulla quasi totalmente nei primi micromentri del rivestimento. Il trattamento termico solitamente usato per togliere il gas dopo la deposizione non ha effetti, indice che il livello di idrogeno incorporato con la deposizione è molto basso quindi il rischio di infragilimento dell'acciaio è molto basso.

La potenziodinamica su bulloni passivati e trattati termicamente evidenzia l'effetto positivo di questi trattamenti: rendono il deposito più nobile e riducono la corrente di corrosione, il film quindi si dissolve più lentamente.

Contents

List of Figures

List of Tables

Chapter 1

Introduction

1.1 Zinc and galvanization

Zinc is the most important electroplated metal for corrosion resistant applications. About half world production is used with this aim. Galvanization is the process of applying a protective zinc layer on steel to prevent corrosion, from Italian scientist Luigi Galvani. Zinc is often used for coating iron, steel and magnesium parts when protection from either atmospheric or indoor corrosion is the primary objective. The zinc film forms a physical barrier against corrosive agents and acts as a sacrificial anode assuring protection of steel parts exposed due to scratch: zinc has a standard reversible potential [-0.76 V/standard hydrogen electrode (SHE)] that is more negative than that of iron (Fe/Fe^{++} -0.44V/SHE). [44] [31] [10]

There are 3 principal galvanize methods:

- Hot-Dip-Galvanization
- Sherardizing
- Electroplating

1.1.1 Hot-Dip-Galvanization

Steel pieces are dipped into molten zinc (about 449°C) to form a zinc layer on the surface. Other elements such as lead are added to the bath to improve fluidity, recycling

and thermal conductivity. The process forms a zinc layer highly bonded to iron; in contact with air, zinc reacts with oxygen, water and carbon dioxide forming zinc oxide (ZnO), hydroxide ($Zn(OH)_2$) and carbonate ($ZnCO_3$). Galvanized steel can be identified by the crystallization patterning on the surface called "spangle".

The hot dip galvanizing process involves dipping of suspended steel articles into a series of cleaning baths prior to dipping the cleaned steel into a bath of molten zinc. The individual steps are described below

- Hot alkaline degreasing

  The first cleaning step, degreasing, is usually a hot alkali solution that removes organic contaminants like dirt, water-based paint, grease and/or oil. After degreasing, the article goes through a water rinse. Any epoxy paints, vinyls, or asphalt coatings must be removed by mechanical means (e.g. grit blasting) before steel is taken to the galvanizer.

- Pickling

  Next the steel is moved to the pickle bath, an acidic solution of either ambient hydrochloric or heated sulfuric, that removes iron oxides and mill scale from the surface of the steel. After pickling, the steel is rinsed again.

- Fluxing

  The steel then moves into the flux tank. The flux of zinc ammonium chloride serves two purposes; first, the lightly acidic solution cleans any remaining iron oxides, and second it provides a protective layer to prevent any iron oxide formation prior to immersion in the galvanizing kettle.

- Hot dip galvanizing

  The true “galvanizing” phase of the process consists of completely immersing the steel in zinc bath at temperature around 450°C with an angle to allow air to escape assuring complete surface contact. Some minutes after complete immersion, the steel reaches the bath temperature and the metallurgical reaction is complete.

- Quenching

  The final step in most hot dip galvanizing processes is a quench to promote passivation of the zinc surface and to control the growth of the zinc-iron alloy layers.

The formation of the galvanized coating on the steel surface is a metallurgical reaction, in that the zinc and steel combine to form a series of hard intermetallic layers, prior to the outside layer being, typically, pure zinc. In a cross-section of a galvanized steel coating we can distinguish the following alloy layers: the γ layer (75% Zn, 25% Fe), the δ layer (90% Zn, 10% Fe), the η layer (94% Zn, 6% Fe), the last pure zinc layer. The steel substrate properties (chemistry, morphology, geometry) influence zinc layer.

Zinc layer protects steel from corrosion in three ways.

- The zinc coating acts as a physical barrier against the penetration of water, oxygen, and atmospheric pollutants isolating the steel from the electrolytes in the environment. Furthermore, zinc corrodes slowly compared with steel.
- The zinc coating cathodically protects the steel from coating imperfections caused by accidental abrasion, cutting, drilling, or bending. Cathodic protection of the steel from corrosion continues until all the zinc is consumed.
- Zinc corrosion byproducts on the surface forms the zinc patina. Zinc oxide is a thin, hard, tenacious layer and is the first step in the progressive development of the protective zinc patina. When the whitish layer of zinc oxide is exposed to freely moving air, the surface reacts with moisture in the atmosphere to form a porous, gelatin-type, grayish-white zinc hydroxide. During dry cycles of exposure, the zinc hydroxide reacts with carbon dioxide in the atmosphere and progresses into a thin, compact, tightly adherent layer of basic zinc carbonate. This progression to zinc carbonate enhances the excellent barrier protection afforded by the galvanized coating. Because the zinc patina is relatively insoluble, it prevents rapid atmospheric corrosion of the zinc on the surface of galvanized steel underneath the patina. [31]

1.1.2 Sherardizing

This is a thermal diffusion process: steel pieces are placed into a barrel with zinc powder, heat (300°C) and motion assure diffusion and formation of alloying of the two metal at the surface. It's useful for little complex part, in particular if hydrogen embrittlement must be avoid. This process assure more uniform and smoother surface improving wear resistance, very important property for part in motion. Often sherardized components are also passivated,in particular with phosphate, to reduce coating reactivity and prevent

white rust (zinc oxide film) or the premature formation of harmful zinc salts on the surface.

1.1.3 Electroplating

Electrochemistry is a powerful tools for working with charge particles like metallic cations: we can use voltage difference as driving force for the deposition of metallic layer from ionic baths. Zinc is one of the first material to be treat with this technique, for this reason the term galvanization is related only to it. In comparison with HDG, this process assures higher control of thickness and composition, higher brightness and density, so better corrosion resistant performance. Due to these properties, electrogalvanized steel became in short time one of the most used material in low corrosive condition like outdoor. Automotive field is one of the most important. In the last decades the introduction of european rule for environmental protection banned using of harmful materials, in particular directive 2000/53/EC of the European Parliament (End of life vehicles) forced developing alternative to cadmium coating and hexavalent chromium conversion which have large employ in automotive field. Electroplated zinc and its alloys are a good answer to these requests and research in this direction continues nowadays. [20] [23]

Many factors influence electrogalvanization, summed up in process parameters (temperature, pH, current, voltage, immersion time) and bath composition.

Without subsequent treatment, electroplated zinc becomes dull gray after exposure to air, so that bright zinc is always given a chromate conversion coating or a coating of a clear lacquer (or both) if a decorative finish is required; topcoat can also improve corrosion protection and friction performance [43]. [17]

1.1.3.1 Process

Basic elements of an electrodeposition system are:

- The external circuit, consisting of a source of current usually dc but some particular techniques use alternate one or impulse, means of conveying this current to the plating tank, and associated instruments such as ammeters, voltmeters, and means of regulating the voltage and current at their appropriate values.

- The negative electrodes or cathodes, which are the material to be plated, called the work, along with means of positioning the workpieces in the plating solution so that contact is made with the current source.

- The plating solution itself, almost always aqueous, called the bath. It's usually contained in a tank for part immersion; in continuous plating a system of pipes and spray nozzles assure complete wetting of the metal sheet with solution. Almost always the bath are corrosive and harmful so all the part in contact with it must be made of appropriate material: often plain mild steel for alkaline solutions, and of steel lined with resistant material for acid solutions, e.g. rubber, various plastics, or even glass or lead. Heater, stirrer or other motion system are employed to control temperature and homogeneity of the bath.

- The positive electrodes, the anodes, usually of the metal being plated but sometimes of a conducting material which serves merely to complete the circuit, called inert or insoluble anodes. [56] [50] [43] [18]

We can distinguish three different systems depending on the piece geometry: barrel, rack and continuous plating.

- Barrel plating typically involves a rotating vessel that tumbles contained workload. The barrel is immersed, sequentially, in a series of chemical process tanks, including plating baths. Utilizing interior cathode electrical contacts to polarize the workload, dissolved metals are attracted out of solution onto each piece. Effectively, the workload becomes part of the plating system during processing because the pieces function as bipolar electrical contacts to the other pieces in the workload. [58] This system is powerful for small pieces to be plated in large quantities, such as fasteners, nuts, bolts, but it is not used for delicate pieces. The time of immersion in the different baths is critical in this process.

- In rack plating pieces are mounted on a rack for the treatments. Racks are fixtures suitable for immersion in the plating solution. The part position is important to obtain a good result: bubble entrapping in the immersion step causes no deposition, furthermore dragged-out bath solution can react with the deposit and worsen the work. [43]

- In continuous plating the pieces move continuously passing either one row or between two rows of anodes. Continuous plating is usually used for pieces of simple and uniform geometry, such as metal strip, wire, and tube. Common product is galvanized steel sheet used for protecting car bodies against corrosion. [43]

  This technique requires close control of current density and hydrodynamic conditions at plating surface to obtain homogeneous deposit. For this reason equipment design and process control become essential. [62] [10]

1.1.3.2 Bath

After the first industrial bath based on cyanide around 1930, in 1960s a more bright zinc is obtained with chloride bath, instead from 1980s also free cyanide alkaline solution are developed and used.

Cyanide bath

Most cyanide baths are prepared from zinc cyanide, sodium cyanide and sodium hydroxide. Common additives are sodium polysulfide acting as a bath purifier against heavy metal precipitation and organic brighteners. Zinc cyanide is practically insoluble in water instead when added to sodium cyanide it dissolves to produce sodium zinc cyanide; on the other hand with sodium hydroxide it yields sodium zincate and sodium cyanide. So in solution we have an equilibrium between all these salts.

The cathode reaction mechanism in cyanide and in alkaline noncyanide baths is similar: cyanide or zincate turns into zinc hydroxide which reduces to metallic zinc.

Bright cyanide zinc baths can be divided into four broad classifications based on their cyanide content: regular cyanide zinc, midcyanide, low-cyanide and microcyanide baths. Regular, mid- and low-cyanide zinc baths behave as cyanide one. The current efficiency decreases with salt concentration, throwing and covering power improve. Instead microcyanide bath is alkaline noncyanide type: cyanide acts as an additive that can be replaced by organic ones. [62]

Alkaline cyanide-free bath

These baths are a logical development in the effort to produce a nontoxic cyanide-free

zinc electrolyte. Various types of deposits could be obtained as a function of current density and solution agitation, in fact also hydrodynamic control is an important factor to have compact layer instead of powder.

These bath are basically solution of zinc and sodium hydroxides. We can distinguish two different ranges of concentrations, low chemistry (LC) and high chemistry (HC), both salt concentrations change. In comparison with cyanide systems, noncyanide alkaline zinc baths have a narrower range of optimum operating zinc concentration. In the first commercial alkaline noncyanide zinc baths, cyanide ions was replaced by other complexing agents like ethylenediamine tetraacetic acid (EDTA), gluconate, tartrate, and triethanolamine. But in this way new effluent problems trouble baths so this approach has fallen out of use, and the alkaline noncyanide zinc baths may now be considered zincate baths. Organic additives are fundamental to obtain good appearance, many compounds act as carrier or brightener; they are usually adsorbed on cathode film hindering metal deposition.

The deposition of zinc takes place through a four-step mechanism: zincate ions lose hydroxide ions and undergo reduction slowly enough to form a dense deposit.

Today zincate plating is a highly successful process being more popular than the cyanide one. [62]

Acid bath

This type of bath radically changed the technology of zinc plating since the early 1970s and constitutes about 50% of all zinc baths for rack-and-barrel plating in most developed nations.

Chloride baths are the most used acid solution. The zinc source is usually zinc chloride. They are principally of two types: with ammonium chloride or with potassium chloride. In the second case is often added also boric acid. Other acid baths like sulfate are used for specific applications. Many organic compound are added to these solution as carriers and brighteners.

Many reactions take place on the cathode surface. Hydrogen evolution involves adsorbed hydrogen atoms and ions. For zinc electrocrystallization, Zn^{+}_{ads} adions diffuse along the electrode surface, undergo reduction with electrons and oxidation with hydrogen ions.

Because of the high values of the exchange current density, organic additives are used to avoid noncoherent deposits. [62]

1.2 Zinc-Nickel plating

1.2.1 Zinc alloy

During the last three decades zinc alloys were introduced with the aim to improve the general behavior of the plate in connection with customer requirements, mainly deformability, weldability, paintability, corrosion resistance after surface conversion and painting, quality finishes and lasting finishes. Research in the field is still very active, the push came mainly from the automotive industry and from the aerospace field in its demand for fastener and electrical components. [57] Today, there is talk to replace cadmium because of its toxic nature. Zinc-nickel is the most common answer for this request. [45] [49] [2] [13]

- Zinc-cobalt alloys are plated from conventional low ammonium or ammonium-free acid chloride baths, with the addition of a small amount of cobalt. Alloys at low cobalt concentration, around 0.3%, show interesting properties, and they have been considered for high-current-density plating in a ternary zinc-nickel-cobalt alloy.

- Zinc-iron alloys are mainly used for their ability to produce a nonsilver black chromate. Zinc-iron alloys were also studied, with the idea of improving phosphatability and paintability, the two weaknesses of zinc-nickel alloys. They are mostly deposited from alkaline baths, sulfate at moderate pH, or chloride.

- Brass (zinc-copper alloy) can be plated from pure zinc to pure copper. It is used in many applications: bright decorative finishing, antique or other dark finishing, as a good drawing lubricant on steel sheet and to provide good adherence of rubber to steel (e.g., steel tire cord wire). Commercial brass plating solutions are cyanide based.

- Zinc-manganese alloys have recently received attention for their extremely high corrosion resistance without the aid of painting, for the formation of dense corrosion

product of γ phase Mn_2O_3 and for their excellent paintability properties. Electroplating needs complexation because zinc and manganese have reversible potentials different by more than 0.4V. [62] [12] [64] [37]

1.2.2 Anomalous deposition

All the zinc alloys with a metal from the iron group (nickel, iron, cobalt) are obtained under so called anomalous codeposition, that is, with preferential deposition of the less noble zinc; however, a normal codeposition can be obtained under particular plating conditions. [10] [7] [34]

One of the possible reasons for anomalous zinc and nickel codeposition is a hindrance in the discharge of nickel ions due to adsorption of zinc hydroxides. These hydroxides are formed as a result of electrolyte alkalization near the cathode surface during the intense hydrogen production. [62] However, it has been shown recently by measuring the pHs values in the vicinity of the cathode surface, that the inhibition in the reduction of nickel ions does not result from the formation of zinc hydroxides; the pHs values not reaching the values needed for hydroxide formation. [11]

These results permit to attribute the anomalous deposition of Zn–Ni alloy to high overpotential of nickel deposition on zinc substrate and peculiarities of the structure of the electric double layer containing the zinc ions together with the nickel ones. In fact thin Zn deposit at a monolayer level formed in the underpotential deposition region inhibits the nucleation growth process of Ni greatly. Moreover zinc ions replace the nickel ions in the dense part of double layer due to the zinc ion's higher surface activity in comparison with the nickel ones. [48] [11]

The model of anomalous codeposition can be used to explain the fact that the microstructure (grain size) in zinc-nickel coatings is finer than that in zinc coatings. Consequently, it is possible to obtain nanocrystalline zinc-nickel coatings. [42] [19] [21]

1.2.3 Phase of plated zinc-nickel

By electroplating it is possible to obtain alloy phases of metastable structure; these phases may be different from those reported for metallurgical equilibrium conditions or may

have different compositions for the solubility limits, in some cases with very important enlargement. In electrocrystallisation of alloys phase selection and formation is the result of non-equilibrium processes, responsible for the suppression of an equilibrium phase or for the formation of a metastable phase. [12]

As we can find in the literature many factors influences phases. The structure of Zn-Ni coatings depends mainly on the Ni content in the alloy, i.e. bath composition (%Ni and %Zn, additive) and all process parameters as voltage, current, agitation can affect the result. [29] [24] [28]

In particular with acidic bath the characteristics of the Zn–Ni alloys were mainly dependent on their composition. [11] With some alkaline electrolytes the phase structure seems more closely related to the hydrodynamic conditions (deposit change drastically with and without agitation system) and to the nature of the amine used as additive. Also alloys with very similar composition show different structure due to process parameters. [46]In other cases galvanostatic conditions imposed on the deposition of the layer determine mainly the structure of the coating. [14]

Among phases of zinc-nickel system, the following ones are involved typically in electrodeposition:

- η: <7%Ni hexagonal structure similar to zinc crystalline structure; the cell parameter exhibits a slight decrease in comparison with that of pure zinc, this can be explained by the replacement of zinc by nickel in the cell.
- δ: $\simeq$11%Ni Ni_3Zn_{22} monoclinic intermetallide; in same case it can be detected only after heat treatment at 250°C.
- γ: from 12% to 25%Ni Ni_5Zn_{21} body centered cubic structure; even if the right concentration is $\simeq$19%Ni, in this range a solution with higher or lower nickel content, so cell parameter changes with it. This is the most interesting phase for its corrosion resistance, much higher than pure zinc.
- α: >70%Ni face centered cubic structure, a solid solution of zinc in nickel.

Out of this range but in same cases also with these concentrations the deposit consists of two phases: in the range 5.0 to 14.0%Ni η and γ, over 25%Ni γ and α, as we can see

with chloride bath. Instead other type of bath like ammonical diphosphate one promotes deposition of homogeneous phase structure. [11] [37] [49] [55] [33] [60]

The micro-morphologies of the coatings can be divided into two microcosmic sizes: nanocrystalline grains and micron-sized colonies. The surface of nanocrystalline grain and colony is rectangular pyramid morphology and nodular morphology respectively. The current density has a strong influence on grain size and surface morphology of Zn–Ni alloy deposits. When the current density is relatively higher, the coatings have the larger colony size and clearer colony boundary but finer grain size on nanoscale. The rapid nucleation rate at high current densities results in the decrease in grain size of deposits. [27] Also nickel content influences morphology structure sizes: the grain size exhibits a decrease as the nickel content increases, i.e. α phases is built of nanocrystallites; instead microcolony size increases with %Ni. [11] [42]

Coating composition changes also with thickness due to variation of nickel content. The concentration of nickel exhibits a drastic decrease with the coating thickness. For coatings thicker than 1 μm the alloy composition remains almost constant. It was also found that the change in the nickel content during the alloy plating is accompanied by a change in the phase composition. Thus, thin coatings with a thickness less than 0.3 μm are mainly formed of amorphous nickel-rich α phase with traces of fine-grained polycrystalline zinc. With higher thickness the deposit is made of zinc rich phases. [11] [21] [41]

1.2.4 Bath

1.2.4.1 Classification

Many baths have been developed for zinc-nickel plating, we can divide them based on pH into alkaline type and acid one. [62] In the first group we have cyanide solution, historically the first system developed. Due to its toxicity many researches have looked for alternative alkaline bath less dangerous for human health and environment, in this way are developed zincate bath and tartrate one. [35] [27] The second group includes chloride bath, usually with ammonium addition, and sulphate one; [53] [63] some studies are done also on ammonical diphosphate electrolyte. [61]

1.2.4.2 Properties

Even if it's possible to obtain similar deposits with both acidic baths and alkaline ones, the solutions have basically different features.

The nickel content of coatings from the alkaline bath is generally not affected by the cathode current density over a wide range of the current density. Therefore, the nickel content on the coating surface should be approximately identical even for a complex shaped part for which the current densities at different zones on the surface of the part are different, so industrial application of the alkaline Zn–Ni electroplating bath. Furthermore, deposition of single phase is simpler. In contrast, the nickel content in the coatings obtained from the acid bath is not constant. Therefore, it is difficult to obtain a single-phase coating. Therefore, the coatings from the acid bath may exhibit generally lower corrosion protection. [42]

In addition, the alkaline zinc–nickel deposition process is less corrosive allowing longer life of the equipment. [35]

1.2.4.3 Components

Plating bath ingredients serve one or more of the following functions: providing a source of the metals being deposited, forming complexes with ions of the depositing metal, improving conductivity, stabilizing solution components and pH, regulating the physical form of the deposit, controlling anode dissolution.

Zinc and nickel source are respective salts: usually zinc oxide and nickel sulfate for alkaline baths, chlorides or sulfates for acid ones.

Additives carry out many functions described above; based on their role or how they work are called brightening, complexing, levelling, grain-refining agent.

The use of additives in electroplating bath is extremely important due to their influence on the growth and structure of the resulting deposits. The presence of additives has been shown to influence physical and mechanical properties of electrodeposits such as grain size, brightness, internal stress, pitting and even composition. A very large variety of organic additives is used, their purpose being to improve the appearance and properties

of the deposits and/or to improve the operating performance of the plating bath. [35] [51]

Complexing agent forms complex with metal cation, in this way they stabilize the ion; presence of the ligand lowers the concentration of the free aquated ion assuring control of the evenness of plating, in fact only complexed ion can discharge at the cathode surface and codeposit. Due to adsorption on cathode surface some agents can work also on the surface. [15] [54]

The cyanide ion, CN^-, is a common ligand forming complex ions for alkaline bath, not only for zinc and nickel. In recent years, many attempts were done to investigate the alkaline non-cyanide bath and a number of complexing agents have been proposed: tartrate, sodiumacetate, many amines (triethanolamine, ethylenediamine), glycinate, citrate, urea, dimethylhydantoin (DMH), N-[1-(2-pyrrolidonyl) ethyl] methyacrylamide (PEAA), triethanolamine (TEA). Also polyligand system containing a mixture of amino acid and alkanolamide are developed. [62] [56] [42] [26] [61] [27] [40]

Brightening, levelling and refining agents usually work directly on the cathode surface by an inhibition effect on the Zn–Ni alloy deposition, by blocking the active sites available for the deposition, due to the additives adsorption on the electrode surface. This inhibition depends on the type and size of the organic molecules and, on the specific interaction between the additives and the substrate. An absorbed layer can form continuously on the surface of the cathode, the deposition occurs only when the zinc and nickel ions arriving at the surface of the cathode can go through this absorbed layer. This delays the movement and discharge of the zinc and nickel ions. As the micro-protrude regions of surfaces have higher current density, the additives tend to absorb preferentially on these areas. The deposition rate of the zinc and nickel on these points can be reduced. As a result, a more even and bright coating can be obtained. [16] [47]

Therefore the morphology is induced by the additives: they lead to smoother and more compact deposits. A fine grain structure and low porosity in Zn–Ni alloy coatings could greatly improve the corrosion resistance. Some compounds can influence the grain shape e.g. inhibiting lateral growth.

Some example of brightening and levelling agent in literature are: sulphanilic acid (SA),

gelatin, tetrakis(2-hydroxyethyl)ethylenediamine (THEED), phenolic derivative, unsaturated aromatic compound, aromatic carboxylate. [46] [35] [42] [22] [63] [3]

Some salts are added to the bath to increase the conductivity and ionic strength of the electrolyte, e.g. NH_4Cl and KCl for chloride solutions.

Among Zn-Ni chloride baths, addition of ammonium chloride or acetate is common, also acid without addition of ammonia or acetate.

In some case bath needs bases or acids to adjust pH value and to assure dissolution of compounds; i.e. in alkaline solutions zinc oxide is dissolved in NaOH solution with pH around 13 before the addition of complexed Ni. [22] [53] [40]

1.2.5 Deposition property: anticorrosion mechanism

Zinc coatings work as sacrificial barrier protecting steel underlying, in this way also scratch, pit or other defects aren't harmful. Adding nickel we can increase the coating nobility, decreasing corrosion current density. As the nickel content rises, the corrosion potentials of the Zn–Ni coatings shift into the positive direction; when nickel exceeds a limit concentration the deposit becomes more noble than the substrate, losing its sacrificial properties. An alloy composition including 10–15% by weight of nickel leads to maximum corrosion resistance. [6]

Nickel slows down the dehydration of the zinc hydroxide, a product of the corrosion, into ZnO. The hydroxide has a lower level of electronic conductivity than the oxide, so the reaction of the cathodic oxygen reduction is weaker than for the oxide, and corrosion is therefore slower. [32]

The corrosion behavior of zinc–nickel coatings depends not only on chemical composition but also on phase composition. The lowest corrosion currents are characteristic of single-phase coatings. The zinc–nickel coating consisting of γ phase exhibits the best corrosion protective properties in a chloride environment. Inhomogeneity in phase composition leads to the degradation of corrosion protective properties of Zn–Ni coatings. This decrease in the corrosion protective abilities can be attributed to the formation of corrosion cells consisting of a two-phase coating. [11] [1]

As zinc coatings, also zinc-nickel ones can be chromated, even if with nickel the deposit becomes more passive and accordingly less receptive to form a good chromate conversion coating. [62]

With regard to the corrosion mechanism of these materials, many researchers agree on the process proposed by Lambert et al. Generally, Zn-Ni alloys are less active than pure zinc, have a lower corrosion velocity and offer less galvanic protection to the steel. The preferential dissolution of zinc at the start of corrosion offers good galvanic protection. However, this leads to Ni enrichment of the alloy and the rise in corrosion potential towards nobler values, thus offering less cathodic protection to the steel. This process is accompanied by progressive structural change, causing phase transformation. Internal stresses increase giving rise to cracks over the whole coating, thus leaving the steel substrate exposed to the environment. The rapid increase in pH inside the cracks, due to the cathodic reduction of oxygen, causes precipitation of corrosion products which fill the cracks. The coating assumes a composite-like structure, formed of corrosion products and an Ni enriched alloy layer. This composite coating acts as protective barrier. [29] [8] [34] [39]

1.2.5.1 Alkaline bath

Basic alkaline baths usually contain zinc and nickel ions, an alkali metal hydroxide and a complexing agent for nickel. Industrial electrolytes contain a family of additives which includes various brighteners and current efficiency promoters. [46] [42]

The electrolyte for the alloy deposition is usually prepared in the following manner. Sodium hydroxide is dissolved in distilled water. The required quantity of zinc oxide is added to the above solution which is then stirred to dissolve the zinc oxide completely. The required quantity of nickel chloride is dissolved in distilled water with complexing agent. Nickel solution is slowly added to the zinc solution with continuous stirring. Then the bath is completed with other additives. Finally the volume of mixed solution is adjusted by adding water. The prepared solution was then filtered. [61]

The pH of the mixed solution is controlled to be above 12 during the deposition, 13 is the optimum value. Complexing agent in the bath has an important role in the dissolution of Ni compound in the alkaline solution. When its amount in the bath is insufficient to

stabilize the metal species the precipitation of metal compounds is observed after mixing the two solutions. [14] [40]

In the following table 1.1 we report composition of some alkaline baths for zinc nickel plating found in literature; most are sodium hydroxide solutions, some are ammonium/ sodium diphosphate ones. [35] [46] [42] [14] [40] [11] [27] [26]

TABLE 1.1: Composition of some alkaline baths found in literature.

Sodium hydroxide baths	
Bath constituent	Optimum concentration
NaOH	380 mM
ZnO	12 mM
$KnaC_4H_4O_6$	110 mM
$NiSO_4{\cdot}6H_2O$	5 mM
NaOH	380 mM
ZnO	12 mM
$KnaC_4H_4O_6$	110 mM
$NiSO_4{\cdot}6H_2O$	5 mM
Brightener	3.7 ml/l
4-methyl benzaldehyde	0.4 ml/l
ZnO	160 mM
$NiSO_4{\cdot}6H_2O$	17 mM
NaOH	3.75 M
Amine	34 mM
THEED	20 g/dm^3
ZnO	12 g/l
$NiSO_4{\cdot}6H_2O$	0.5-4.0 g/l
Heliotropin	0.5 g/l
NaOH	120 g/l
PEAA	30 g/l
Additive	0-14 g/l

Table 1.1: It continues on the next page.

Table 1.1: It continues from the previous page.

ZnO	13 g/l
$NiSO_4 \cdot 6H_2O$	4.5 g/l
NaOH	150 g/l
DETA	3.5 g/l
THEED	20 g/l
NaOH	110 g/l
TEA	50 g/l
Ni	1.0 g/l
Zn	13 g/l
Ammonium and sodium diphosphate baths	
Bath constituent	Optimum concentration
ZnO	0.15 M
NaCl	0.05 M
NH_4Cl	3.0 M
$Na_4P_2O_7 \cdot 10H_2O$	0.3 M
$ZnSO_4 \cdot 7H_2O$	70 g/L
$NiSO_4 \cdot 6H_2O$	30 g/L
$Na_4P_2O_7 \cdot 10H_2O$	40 g/L
DMH	140 g/L
K_2CO_3	95 g/L
Additives	0.04 g/L

Table 1.1: It ends from previous page.

1.2.5.2 Acidic bath

Basic acidic baths usually contain zinc and nickel ions from chlorides or sulfates, ammonium chloride and sodium sulfate as electrolyte, boric acid or other controls solution pH. Industrial baths contain a family of additives which includes various brighteners, complexing agents and current efficiency promoters.

In the following table 1.2 we report composition of some acidic baths for zinc nickel plating found in literature; most are chloride solutions, some are sulfate ones. [11] [22] [53] [3] [63] [48]

Table 1.2: Composition of some acidic baths found in literature.

Weak acid chloride baths	
Bath constituent	Optimum concentration
$ZnCl_2$	0.15 M
$NiCl_2$	0.30 M
NH_4Cl	3.0 M
$ZnCl_2$	0.37 M
$NiCl_2$	0.34 M
NH4Cl	2.24 M
KCl	1.61 M
$C_6H_7NO_3S$	0.03 M
Gelatin	7 g/L
$ZnCl_2$	50-200 g/l
$NiCl_2$ 6H2O	50-200 g/l
H_3BO_3	40 g/l
$ZnCl_2$	135 g/l
$NiCl_2$	142 g/l
H_3BO_3	30 g/l
NaCl	156 g/l
$ZnCl_2$	0.5 M
$NiCl_2$	0.25-1.25 M
H_3BO_3	0.5 M
NH_4Cl	1 M
KCl	2 M

Table 1.2: It continues on the next page.

Table 1.2: It continues from the previous page.

Sulfate baths	
Bath constituent	Optimum concentration
$NiSO_4$	0.2 M
$ZnSO_4$	0.5 M
H_3BO_3	0.32 M
NH_4Cl	0.26 M
Na_2SO_4	1.13 M
$NiSO_4$	2.5 g/l
$ZnSO_4$	1.0 g/l
Na_2SO_4	1.0 g/l

Table 1.2: It ends from previous page.

Chapter 2

Instruments

2.1 Deposit characterization

2.1.1 X-Ray Diffraction Spectroscopy

X-Ray diffraction is based on a three dimensional extension diffraction and interference phenomenon: when two light beam with the same wavelength but a different phase are combined the resulting light intensity isn't homogeneous and a series of peaks and valley is detected. Phase difference may derive by a different path distance.

Considering a crystal, it is composed by special ordered atoms and families of planes (i.e. series of planes parallel and equally spaced each other) are recognizable. As shown in figure 2.1, the incident X-Ray beam is partially reflected and transmitted by all the planes of the family. There is a difference in optical path of the two reflected beam related to interplanar distance d. That results is a phase difference that set up diffraction phenomena. This is possible only with X-Ray light because it has wavelength in the order of Å that is comparable with interplanar distance. In addition, when the phase difference is a multiple of the wavelength, constructive interference (i.e. the resulting intensity is higher than the mathematical sum of the intensity of the beams involved) occurs and a peak is visible. Introducing the Bragg law:

$$2dsen\theta = n\lambda$$

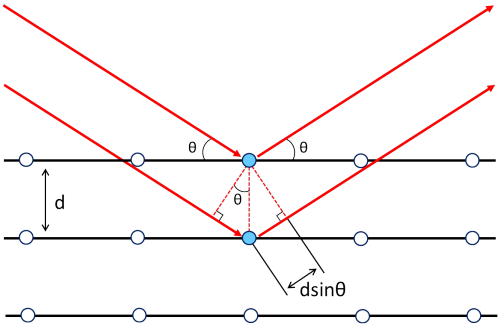

FIGURE 2.1: *Incident beam is partially reflected by each crystalline planes generating a series of reflected beams with different phase due to the different optical path; the superposition of these beams leads to constructive diffraction only when the phase difference is integer multiple of wavelength.*

Wavelength (λ) and interplanar distance (d), that are fixed, are related by the incident beam angle (θ). Continuously changing this angle, reflected intensity peaks are obtained only with θ values that satisfy Bragg law. A 3D pattern of peaks that correspond to different families of planes (with differ d) is obtained and crystalline structure is estimated.

X-ray diffraction measurements of thin films (µm) using conventional $\theta/2\theta$ scanning methods generally produces a week signal from the film and an intense signal from the substrate. One of the ways to avoid intense signal from the substrate and get stronger signal from the film itself is to perform a 2θ scan with a fixed grazing angle of incidence, popularly known as GIXRD. The fixed angle is generally chosen to be slightly above the critical angle for total reflection of the film material.

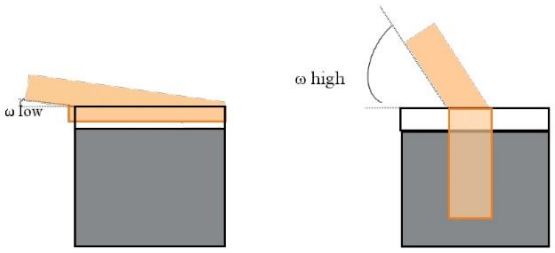

FIGURE 2.2: *In the case of very thin films the scattering volume of the layer will become smaller and smaller as scan progresses to higher angles, the substrate pattern will dominate the diffractogram and could complicate the pattern analysis.*

2.1.2 Scanning Electrons Microscopy

A scanning electron microscope is electron microscope that produces images by scanning the sample. With this technique is possible to obtain topography and composition information depending on the output signal analyzed. As shown in figure 2.3, the instrument could be divided in two main section: electron beam (input) generation and emitted signals (output) detection systems.

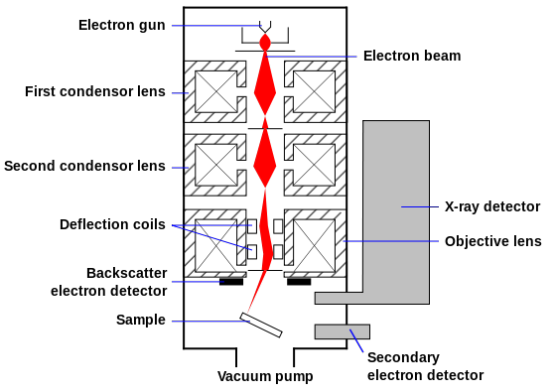

FIGURE 2.3: *SEM apparatus is composed by an electron gun that generates the electron beam, a series of magnetic coils that focus the beam on the sample; after interaction with the sample, the outputs are detected by a series of different detectors depending on the nature of the output signal.*

In the standard configuration, an electron gun thermoionically emits an electron beam that is subsequently focused and collimated by a series of magnetic coils that act for electrons as optical lens act for light beam. Deflection coils deflect the beam in the x and y axes: usually a rectangular portion of sample is scanned. SAMM microscopy is equipped with a LaB_6 that assure a limit resolution of 1,5nm in high vacuum condition, the resolution decreases with lower vacuum.

When the electron beam probes the sample, electrons penetrate inside it and may interact with atoms in two different scattering way: elastic scattering, when electron changes its trajectory without losing energy, and anaelastic scattering, when electron losses energy. These reactions take place inside a certain volume defined interaction volume (see figure 2.4). In case of elastic scattering, an electron collides with atoms and it is re-emitted (backscattered electron). Considering anaelastic scattering, electron looses a part of its energy and it result in emission of secondary electron or X-ray photon. Due to its lower energy, secondary electron is emitted only if it is generated near the surface, otherwise it is reabsorbed by the sample.

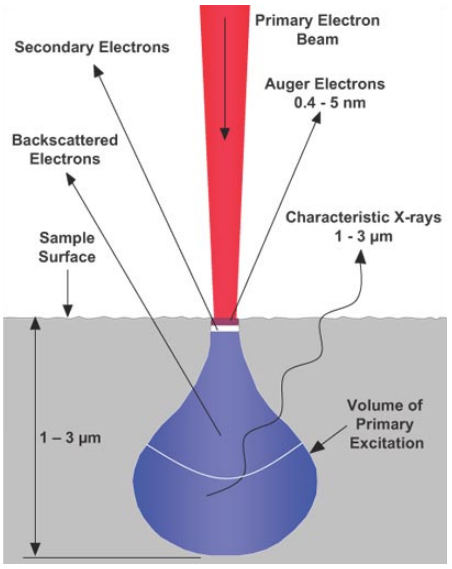

FIGURE 2.4: *All the interaction between electron beam and sample occur inside a portion of volume that depends on material (i.e. atomic number) and energy and angle of incidence of the beam; this volume may be further divide depending on kinds of output (higher the energy, deeper the emission zone.*

Measuring intensity and energy of BSE and SE, information about composition and morphology are obtained. Varying the energy of incident electron beam, interaction volume is modified and also the SEM image resolution. Different types of generated electrons are detected by specific detectors (i.e.: solid-state or Everhart-Thornley detectors). Energy-dispersive X-ray spectroscopy (EDS) detector assure chemical analysis by means of X-ray photon investigation. In order to balance surface charges, samples must be conductive or plated with metal (e.g. Gold) in order to provide the needed conductivity.

2.1.3 X-Ray Fluorescence Spectroscopy

X-ray fluorescence (XRF) analysis is a non-destructive methods for qualitative as well as quantitative determination of elemental composition of materials. It is suitable for solids, liquids as well as powders. Detection limit depends upon the specific element and the sample matrix but in general heavier elements have higher detection limit.

When a beam of X-ray photons like those produced from an X-ray tube falls onto a sample, a number of different processes may occur. The coming X-ray can either be absorbed (photoelectric effect, Auger effect) or scattered through the material with (Compton effect-incoherent) or without (Rayleigh effect- coherent) loss of energy.

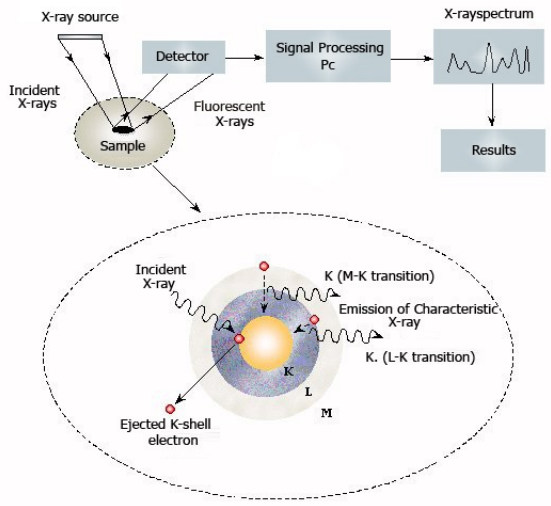

FIGURE 2.5: *XRF physical principle and typical detection arrangement for the analysis.*

If the primary energy of X-rays is equal to or is larger than the binding energy of an inner shell electron it is likely that electrons will be ejected and consequently vacancies are created. The hole state has certain life time and becomes refilled again. The transition of the excited atom into a state with lower energy occurs via two competitive processes, the above mentioned photoelectric and Auger effects. In the photoelectric effect, the recombination is accompanied by a transfer of electrons from the outer shells into the inner shells filling the vacancies. This process induces the emission of a characteristic X-ray (fluorescence) photon. Therefore the energy of these secondary X-rays is the difference between the binding energies of the corresponding shells.

The excited atom can also recombine by emission of Auger electrons, instead of characteristic X-rays, via the Auger effect. The probability that characteristic X-rays will be emitted - and not an Auger electron- varies from one element to another and is described as the fluorescence yield. For elements of low atomic numbers, the Auger effect dominates, whereas emission of characteristic X-rays is more likely for heavy elements. Each element has its unique characteristic energy spectrum (fluorescence spectrum) composed by the allowed transitions of the specific atom in the result of X-ray excitation. XRF technique consists on the study of the produced characteristic spectrum (see figure 2.5) [5]

2.1.4 Glow Discharge Optical Emission Spectroscopy

Glow Discharge Optical Emission Spectroscopy (GDOES) provides rapid, direct bulk analysis and depth profiling analysis of solids. Both conductive and non-conductive layers can be characterized. This technique combines a DC/RF plasma source, chosen in basis of sample material, with optical spectrometer (see figure 2.6).

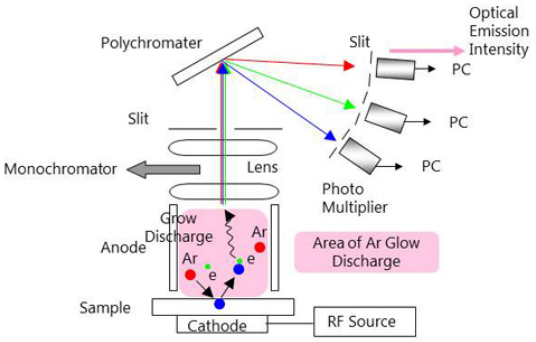

FIGURE 2.6: *GDOES arrangement and principle of operation: sputtering of sample atoms, excitation by means of a plasma, photon detection and analysis.*

In a glow discharge, cathodic sputtering by Argon ion is used to remove material layer by layer from the sample surface. The atoms, removed from the sample surface, migrate into the plasma in proximity of the specimen where they are excited through collisions with electrons or metastable carrier gas atoms. The characteristic spectrum emitted by this excited atoms is measured by optical emission spectrometer. The intensities are recorded as function of time. Based on a calibration method, establish beforehand, these qualitative results can be transformed in a quantitative content depth profile.

2.1.5 Potentiodynamic polarization

A polarization curve is a plot of current density (i) versus electrode potential (E) for a specific electrode-electrolyte combination. It is the basic kinetic law for any electrochemical reaction.

The potentiodynamic polarization technique is generally used to produce a qualitative picture or "fingerprint" of a substance in a given solution. As shown in figure 2.7 it detects important information such as the potential region over which the specimen remains passive, the corrosion rate in the passive region, the ability of the material to spontaneously passivate in the particular medium.

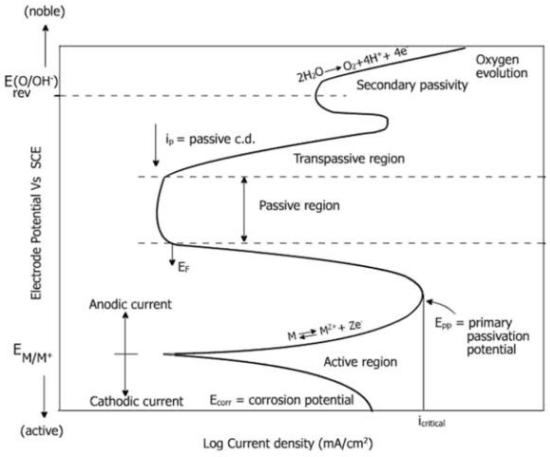

FIGURE 2.7: *Typical polarization curve of a metal: we can recognize active, passive and transpassive region in the anodic branch, a peak indicates anodic-cathodic transition at the corrosion potential.*

Often, polarization curves are plotted in which log $|i|$ is given along the abscissa, even though it is the electrode potential (E) and not the current which is the independent variable. Today most polarization curves are determined potentiostatically: we scan a range of voltage that includes corrosion potential so the sample at the beginning works as cathode then as anode. Semilogarithmic scale highlights corrosion beginning point with horizontal peak: high voltage and low current indicate good resistance against corrosion.

2.2 Bath characterization

2.2.1 Cyclic voltammetry

Voltammetry is one of the electrochemical techniques to investigate redox reactions. As shown in figure 2.8, this analysis is usually performed with a 3-electrode cell: an external electrical circuit connects working, counter and reference electrode, supplies voltage and monitors flowing current.

There are numerous forms of voltammetry: potential step, linear sweep, cyclic voltammetry; for each of these cases particular voltage series are applied to the electrode and the analysis of the current that flows show different properties of the solution.

Cyclic voltammetry in particular is a useful analysis technique used to study redox reactions that happens into a solution. This kind of reactions take place at precise voltage values and involves electrons transfer so positive or negative currents are generated. In

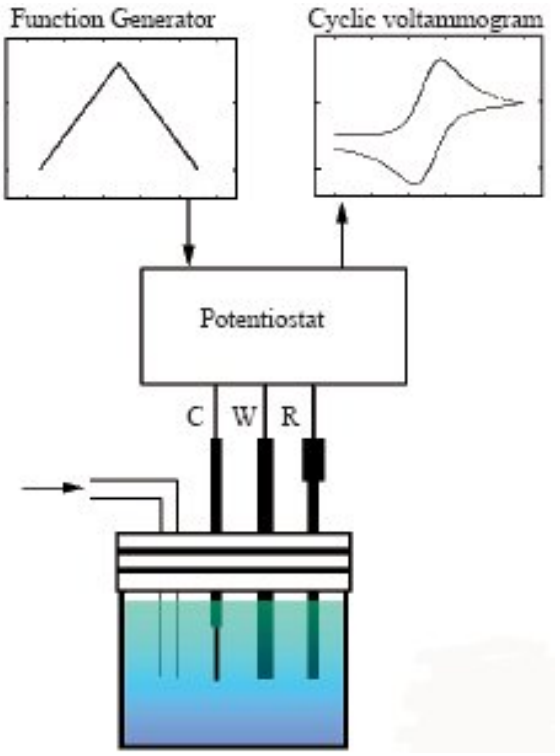

FIGURE 2.8: *Cyclic voltammetry equipment: electrolytic cell with 3 electrodes (W: working, C: counter, R: reference) connected to potentiostat that imposes a particular voltage series and records voltammogram.*

this case the voltage is swept between two values at a fixed rate, when the voltage reaches the second value (in our test it's the minimum) the scan is reversed and the voltage is swept back to the initial value. Voltage increment rate is very slow in order to allow all the reaction and transition to the cell.

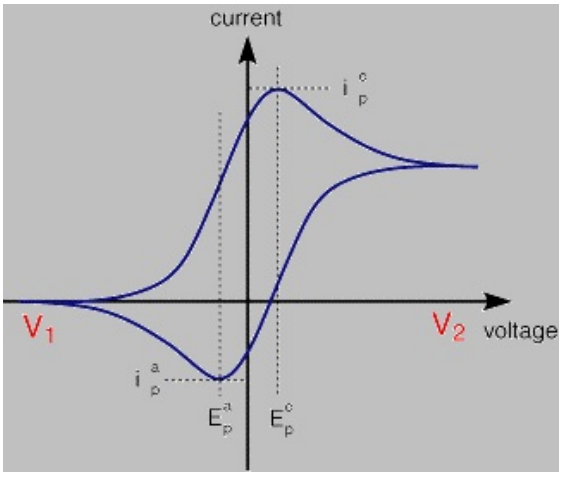

FIGURE 2.9: *Typical cyclic voltammetry curve: we can recognize voltage limit V_1 and V_2, anodic peak and cathodic one.*

The result is a voltammogram made up of two branches, as shown in figure 2.9. The

first is related to reduction of ions in solution, so negative peaks indicated the deposition of a particular phase on the working electrode. The second branch shows the oxidation reactions, the positive peaks are related to dissolution of the previously formed phases. Analyzing intensity and position of current peaks, it's possible to recognize and quantify the reactions that take place and the phases involved.

The characteristics of the voltammogram depend on a number of factors including: rate of the electron transfer reaction, chemical reactivity of the electroactive species, voltage scan rate. [4] [52]

Chapter 3

Experimental analysis

3.1 Deposition study

At the beginning we study the deposition obtained with two different solutions: an acidic bath and an alkaline one. We focus the attention on the effects of voltage and current on the composition of the deposited film.

The final aim of this section is finding the setting to deposit 10µm layer with a content of Ni of about 15%, that is the common content used for typical applications.

3.1.1 Solutions

This thesis is born of a collaboration with GLOMAX s.r.l., interested in studying more thoroughly the behaviour of its products. Therefore in the analysis we focus attention on baths that they supplied us.

3.1.1.1 Acidic solution

Table 3.1 shows the composition of acidic bath ECOLUX STEEL^{TM} [30]. It's a typical chloride acid solution for zinc-nickel plating with 4 additives, each one has a specific function:

- ECOLUX STEEL A: it's the base additive, it works as leveling and grain-refining agent. It also assures good deposition with a broad range of potential.

- ECOLUX STEEL B: it works as brigthening agent, it has only an aesthetic effect and it doesn't influence phase composition.
- ECOLUX STEEL C: it works as complexing agent, it keeps in solution metal ions and controls their deposition assuring bright deposit and clear bath.
- ECOLUX STEEL D: it maintains uniform distribution of Ni^{++} ions during whole service life.

TABLE 3.1: Composition of ECOLUX STEEL™

Compound	Range	Optimum
Metal Zinc	22-30 g/l	26 g/l
Zinc chloride		55 g/l
Metal Nickel	22-30 g/l	26 g/l
Nickel chloride · $6H_2O$		105 g/l
Potassium chloride	160–200 g/l	180 g/l
Ammonium chloride	45-75 g/l	60 g/l
ECOLUX STEEL A	10–20 ml/l	15 ml/l
ECOLUX STEEL C	10-20 ml/l	15 ml/l
ECOLUX STEEL B	1-2 ml/l	1 ml/l
ECOLUX STEEL D	4-6 ml/l	5 ml/l

3.1.1.2 Alkaline solution

Table 3.2 shows the composition of alkaline bath GLOVEL 800™.

TABLE 3.2: Composition of GLOVEL 800™.

Compound	Range	Optimum
Metal Zinc	9–15 g/l	12 g/l
Metal Nickel	1-2 g/l	1.5 g/l
Sodium hydroxide	120-140 g/l	130 g/l
GLOVEL 800 A	60-100 ml/l	80 ml/l
GLOVEL 800 B	1-2 ml/l	1.5 ml/l
Additivo Ni b.d.c.	4–8 ml/l	6 ml/l
Complex Ni	10-20 ml/l	15 ml/l

It's a typical sodium hydroxide solution for zinc-nickel plating with 4 additives, each one has a specific function:

- GLOVEL 800 A: it's the base additive, it works as leveling and grain-refining agent. It also assures good deposition with a broad range of potential; it is essential to dissolve nickel as we see during the test.

- GLOVEL 800 B: it works as brigthening agent, it has only an aesthetic effect and it doesn't influence phase composition.
- Additivo Ni b.d.c.: it maintains uniform distribution of Ni^{++} ions avoiding tendency to concentrate at the bottom of the bath.
- Complex Ni: it works as complexing agent, it keeps in solution metal ions and controls their deposition assuring bright deposit and clear bath.

3.1.2 Substrate

The most common application for tested baths is the treatment of steel parts so we chose as substrate a simple steel sheet. We cut the sheet to obtain samples 7 cm high and 1,5 cm wide. This size is convenience for our tests: it is big enough to have 1 cm^2 for deposition and small enough to assure good accommodation into the beaker used as bath tank.

A protective zinc oxide layer cover the surface against corrosion, so it requires a pretreatment: each piece is dipped in concentrate hydrochloric acid solution to remove this film, in this way we obtain a clean and mirror like surface.

After water rinsing and drying, the sample is covered with Kapton tape in order to leave free on one side a window of 1 cm^2: in this way we have a deposition area convenience for current calculation.

3.1.3 Cell and equipment

We use a power supplier to deposit our samples and EG&G potentiostat/galvanostat model 273A to study the behavior of baths and samples.

With the first instrument we use a two electrodes configuration. Steel sample is connected to the negative pole working as cathode. After some tests with platinum plated wire and De Nora^{TM} mesh as anode, we decide to connect to the positive pole a zinc piece: in this way we assure zinc ion replacement during plating. Filter paper package wraps zinc anode reducing contamination of the bath and assuring longer service life. We can supply power in two way: potentiostatically imposing a particular voltage difference between

the poles or galvanostatically controlling current. We control deposition time by means of a chronometer.

EG&G assures higher control. It uses three electrodes configuration: steel sample as working electrode, zinc piece with filter paper as counter electrode and saturated calomel electrode (SCE) as reference electrode. This electrode is based on equilibrium of mercury chloride, called calomel, kept in a saturated solution of potassium chloride that provide chloride ions. Its equilibrium potential is E=+0,241V respect to the standard hydrogen electrode. We can choose both potentiostatic condition, imposing the potential of the working electrode respect to the reference one, and galvanostatic condition. By means power suite pc software, we can set value and time of current/potential imposed to working electrode.

The cell set up is:

- a beaker as bath tank
- electrodes in the following geometry: free area of steel sample is opposite to the zinc piece, reference electrode is next to the sample with the porous salt bridge near the free area in order to assure accurate potential measurement without hindering ion flux
- a system of clamps and stands to fix electrodes

Temperature, pH and stirring are the most important bath parameters that can influence deposition. Temperature control is obtained by using a heater device with an integrated stirring system and pH is evaluated by a pH-meter. PH is corrected in the required range by addition of concentrate acid (5% sulfuric acid to low pH) or a base (1 M caustic soda to increase pH).

We use about 100 ml of solution; in this way the free area of the steel sample is completely wet by the bath, instead the other side with electrical contact is out avoiding unwanted short circuit.

Due to small deposition area and thin layer, metal ion consumption is low; furthermore contamination sources are almost absent so we can reuse several times the same solution.

3.1.4 X-Ray fluorescence spectroscopy

After the deposition step, each sample is rinsed with water to eliminate solution excess that can damage the deposit, and dried.

Then we control uniformity, possible border effect and aesthetical appearance of the deposit by a visual examination: our purpose is to obtain homogeneous bright grey film first.

Then XRF give us quantitative information about layer thickness and composition, i.e. Ni and Zn content. After setting the machine through a program prepared specifically for our sample type (zinc-nickel layer onto steel substrate), it takes 30 seconds to examine a micro area. We analyse 4-5 points for each sample to evaluate composition distribution.

3.1.5 Deposition test

3.1.5.1 Optimized deposition for acidic solutions

We start analysing complete ECOLUX STEEL^{TM} bath and the basic version containing only salts without additives; samples from first bath are marked with letter A, those from the second one with letter B.

First aim of the deposition test is to find optimal deposition set up to obtain a 10 μm thick film with a nickel content from 14% to 16%.

Temperature and pH must fall into a range near optimal value as indicated in table 3.3.

Table 3.3: Optimal value of temperature and pH for bath A and B.

	Temperature	pH
Bath A	30-35°	5.0 - 5.5
Bath B	30-35°	4.5

We use stirring during deposition to promote solution mixing in order to avoid composition gradient close to cathode surface and into the bath.

Cyclic voltammetry suggests us potential range for a good deposition. We do many tests with both power supplier and the EG&G potentiostat/galvanostat, both in potential

control and in current one. Optimal parameters are used to prepare samples for SEM and GDOES analysis.

Data of best samples are summarized in table 3.4.

TABLE 3.4: Optimal deposition parameters and relative XRF analysis.

Control	Sample	Deposition parameters			XRF data		
		Potential (V vs SCE)	Current density (mA/cm^2)	Time (min)	Thickness (μm)	%Ni	%Zn
Potential	A44	-1.5		6	9.645	14.4	85.6
	B17	-1.4		5	7.575	14.45	85.55
Current	A46		25	25	10.7	15.7	84.3
	B30		35	13	10.8	15	85

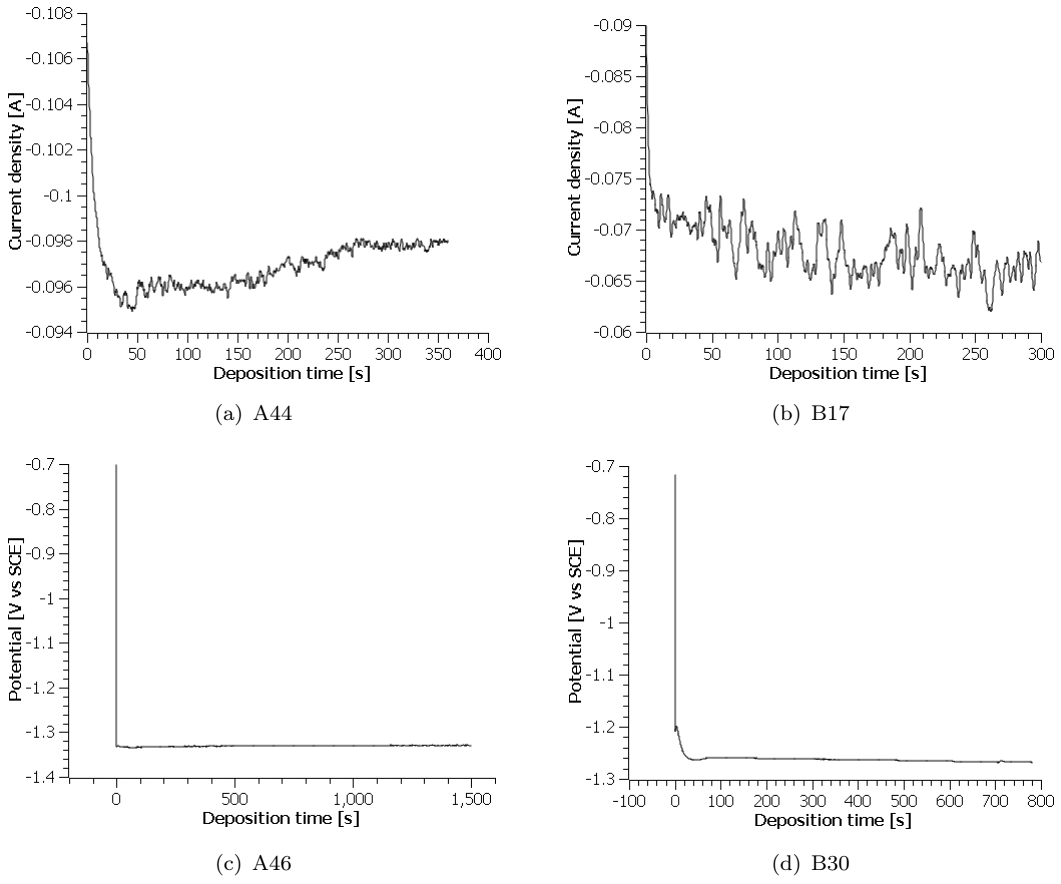

(a) A44 (b) B17

(c) A46 (d) B30

FIGURE 3.1: Current or potential variation during deposition with EGeG.

All these samples are obtained with EG&G system so with a more accurate way to set current density or potential. In this way we can study the evolution of free variable (current density for samples A44 and B17, potential for samples A46 and B30) during the deposition (figure 3.1).

- A44: Current starts at 107 mA, then it falls to 95 mA in the first 30 seconds due to formation of less conductive plated layer; during deposition it slowly raises and stabilises at about 98 mA.
- B17: Current falls from 90 to 75 mA, then decreases slowly till 65 mA due to layer growth. Causes of instability of the signal can be excessive stirring and formation of pits and cracks, preferential path for current.
- A46: Equilibrium potential of steel into the bath is -0.7 V vs SCE; when current is applied, potential falls instantly to -1.33 V and it remains constant during all deposition time.
- B30: Equilibrium potential is about -0.7 V as previous sample, it falls to -1.26 V in the first 30 seconds then it decreases slowly till -1.27 V during deposition.

Comparing these graphs, samples A44 and A46 present a more stable signal respect samples B17 and B30; it's additives effect: they control ion transfer so signal suffer less volatility.

3.1.5.2 Effects of deposition parameter

Potential To understand how potential influences the deposit composition and its thickness, we do a series of potentiostatic deposition with both the baths. We use the optimal parameters varying only the potential (±0,05/0,1 V) around -1,5 V for solution A and -1,4 V for solution B. Then we analyse changes of thickness, content of nickel and zinc. Tables 3.5 and 3.6 summarize the results.

Table 3.5: Potentiostatic depositions with bath A around -1,5 V vs SCE to study parameter effects.

Sample	Deposition parameters		XRF data		
	Potential (V vs SCE)	Time (min)	Thickness (μm)	%Ni	%Zn
A43	-1,4	6	5,91	14,8	85,2
A42	-1,45	6	7,565	14,25	85,75
A44	-1,5	6	9,645	14,4	85,6
A40	-1,55	6	10,45	13,9	86,1
A41	-1,6	6	13	14,1	85,9

TABLE 3.6: Potentiostatic depositions with bath B around -1,4 V vs SCE to study parameter effects.

Sample	Deposition parameters		XRF data		
	Potential (V vs SCE)	Time (min)	Thickness (µm)	%Ni	%Zn
B22	-1,3	5	5,7	12,4	87,6
B20	-1,35	5	6,7	14,5	85,5
B24	-1,4	5	7,7	17,6	82,2
B21	-1,45	5	8,9	19,7	80,3
B23	-1,5	5	10	19,9	80,1

Potential has clear effect on thickness: for both the baths growth rate has a linear relation with potential as figure 3.2 highlights, in fact higher driving force assures higher current and in consequence faster plating.

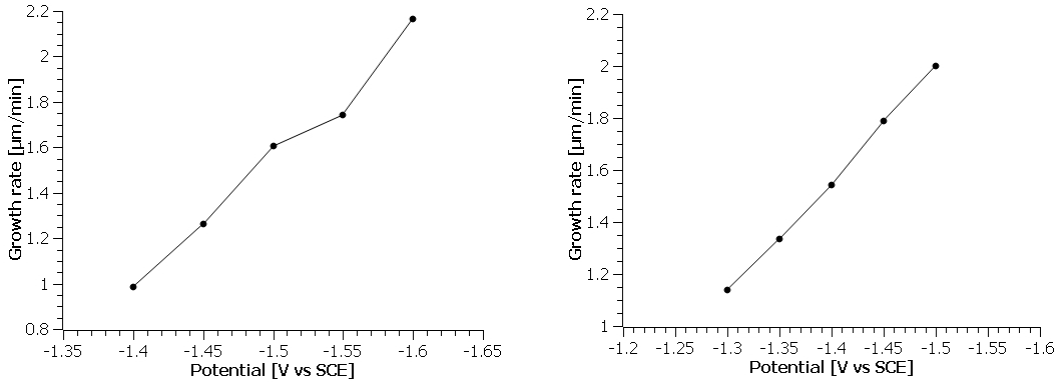

(a) A samples (b) B samples

FIGURE 3.2: Variation of growth rate with potential around optimal deposition value.

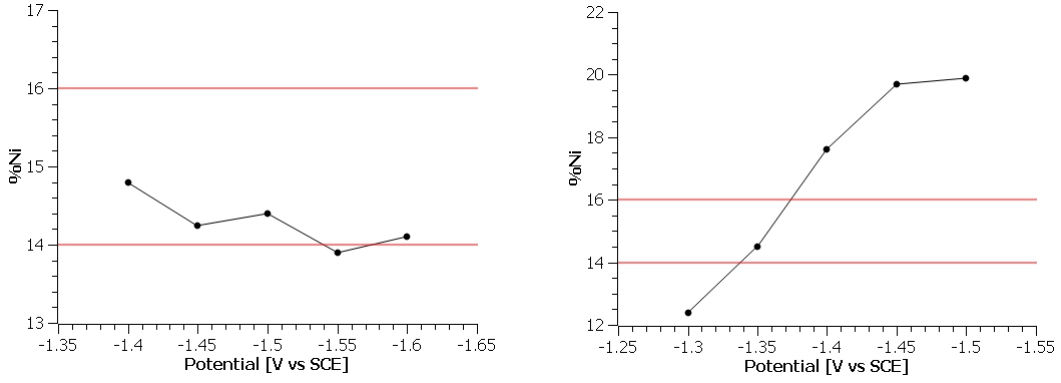

(a) A samples (b) B samples

FIGURE 3.3: Variation of nickel content with potential around optimal deposition value.

Instead potential effect on composition depends on the presence of additives as figure 3.3 shows. In bath B, content of nickel growth with potential; this relation is almost linear till -1,45 V then the slope decreases. [63] [27]

In bath A there isn't a clear tendency: nickel content decreases a bit at higher potential but the most important fact is that additives are able to keep composition into optimal value (14-16%Ni) for a very wide potential range assuring good result in industrial application.

Stirring During most of the depositions, we use agitation but we do also some tests without stirring to observe its effect.

For A solution we can compare three pairs of samples: A37-A45, A22-A23, A33-A34 showed in table 3.7; in each couple first sample is obtained with stirring, the second one without agitation.

Table 3.7: Comparison of A samples for stirring effect investigation.

Sample	Deposition parameters		XRF data		
	Current (mA/cm^2)	Time (min)	Thickness (μm)	%Ni	%Zn
A37	25	21	10,9	12,4	87,6
A45	25	21	8,4	16	84
A22	125	4	9,1	7,92	92,08
A23	125	4	10,0	9,07	90,93
A33	240	1,5	7,35	12,4	87,6
A34	240	1,5	7,32	15	85

Stirring influences clearly the composition of layer: nickel content decreases when agitation system is on. This behaviour can be explained by the presence of fresh solution on the cathode surface thanks to agitation, so zinc ion concentration in the double layer doesn't decrease and in consequence deposit contains less nickel. Considering thickness, only the first pair shows clear variation: A37 is 2.5 μm thicker than A45. Stirring avoid depletion of metal ions near the cathode and long deposition time (21 min) highlights this effect. [27]

For B solution we can compare sample B17 with B18 and B19; deposition parameters are the same, the only difference is presence of stirring during B17 deposition. As table 3.8 shows, stirring has no effects on growth rate, in fact thickness of the sample are similar.

Instead it influences composition: stirring causes depletion of nickel in the deposit as observed in A samples.

TABLE 3.8: Comparison of B samples for stirring effect investigation.

Sample	Deposition parameters		XRF data		
	Potential (V vs SCE)	Time (min)	Thickness (µm)	%Ni	%Zn
B17	-1,4	5	7,575	14,45	85,55
B18	-1,4	5	7,3	17,5	82,5
B19	-1,4	5	7,495	18,85	81,15

3.1.5.3 High current deposition

We do some tests over density current limit indicated for ECOLUX STEEL^{TM}. As we can see in figure 3.4 bath present a regular behaviour till 100 mA/cm^2: growth rate increases linearly instead nickel content is around 9%, below optimal values.

Beyond this limit, data are variable: in these conditions additives don't work as we intended, in fact as highlighted in figure 3.4 only two samples fall into the optimal composition range. So for our purpose it's useless continue in this way.

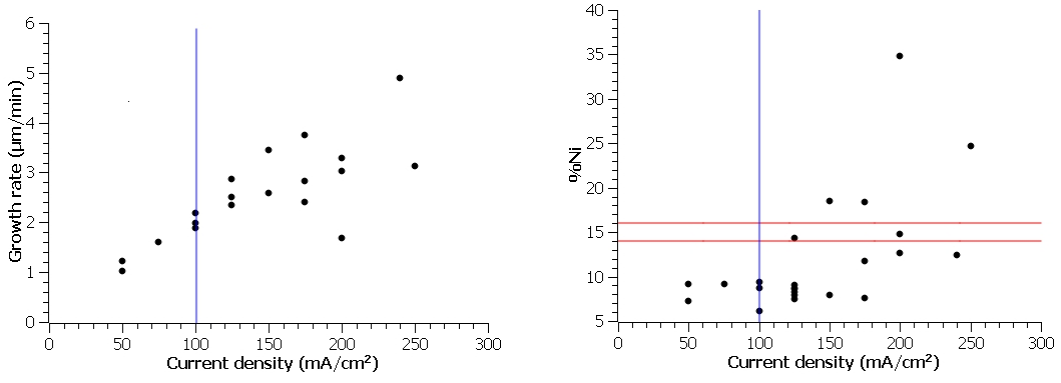

(a) Growth rate (b) Ni content

FIGURE 3.4: Distribution of growth rate and nickel content of samples obtained with high currents.

3.1.5.4 Deposition with alkaline baths

Alkaline solutions are alternative process for zinc-nickel plating, so a comparison with acidic baths can be interesting.

We consider GLOVEL 800^{TM}, a GLOMAX s.r.l. product; we seek parameters for optimal deposition to analyse plated layer with XRD and we try to do cyclic voltammetry in order to observe the effect of additives. We also consider another industrial alkaline bath for a comparison. Sample obtained with these solutions are labeled with letter C (GLOVEL 800^{TM}) and D (other commercial bath).

As we have done with acidic solution, we look for optimal deposition parameters by means plating tests both in potential control and in current control. Table 3.9 shows the results.

TABLE 3.9: Optimal deposition parameters for alkaline baths.

Sample	Deposition parameters		XRF data		
	Potential (V vs SCE)	Time (min)	Thickness (µm)	%Ni	%Zn
C10	-1,6	120	11,4	13,2	86,8
D1	-1,6	110	8,93	14,5	85,5

Potential is a bit lower than that used for acidic bath with additives. Deposition takes longer time due to low growth rate, in fact alkaline baths display lower current efficiency compared to acidic ones. [27]

Figure 3.5 depicts current density effect on properties of deposit obtained with bath C. Growth rate increases almost linearly with current due to increasing driving force. Instead nickel content increases from 13% to 17% at 15 mA/cm^2, then it maintains this value till 45 mA/cm^2. So additives work well keeping deposit composition near optimal range.

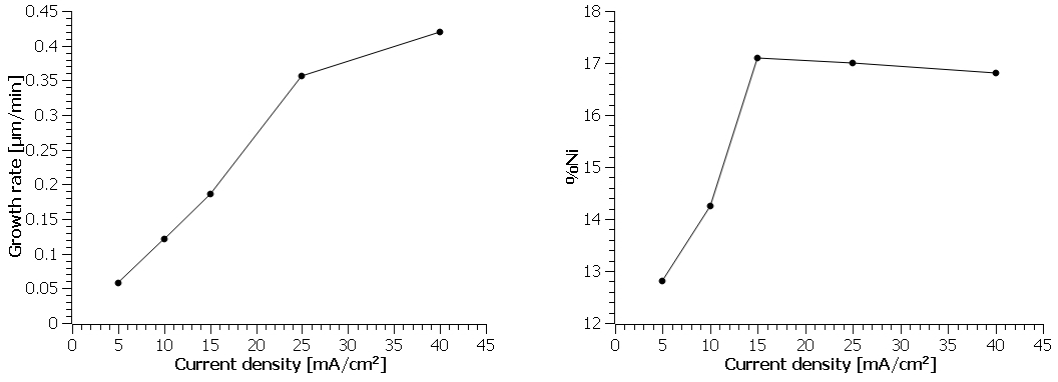

(a) Growth rate (b) Ni content

FIGURE 3.5: Variation of growth rate and nickel content with current.

As we have done with acidic baths, we try to test GLOVEL 800^{TM} solution without additives to understand their effect with deposition test and cyclic voltammetry.

As first attempt, we avoid all additives (GLOVEL 800 A, GLOVEL 800 B and Additivo Ni b.d.c.). We dissolve sodium hydroxide in water, we add zinc oxide and finally, after cooling below 30°T, Complex Ni as source of nickel ions. But this solution suffer of instability, it's cloudy and a sediment at the bottom appears without agitation. Ions can't stay in solution, in particular nickel: in fact deposited layer (sample C11 in table 3.10) shows depletion of this metal. Addition of GLOVEL 800 A doesn't solve instability bath problem and deposit appearance isn't good (sample C12).

TABLE 3.10: Information of samples obtained with GLOVEL 800^{TM} bath without additives.

Sample	Deposition parameters		XRF data		
	Potential (V vs SCE)	Time (min)	Thickness (μm)	%Ni	%Zn
C11	-1,6	10	1,7	10,4	89,6
C12	-1,6	10	0,76	22,8	77,2

GLOVEL 800 A must be premixed to solution with Complex Ni and then all can be added to alkaline zinc solution: in this way GLOVEL 800 A perform its function to stabilize the bath. In order to this a right ratio between GLOVEL 800 A and Complex Ni must be maintained inside the bath: below a ratio of 5:1 the stability will be lost, the result is a solution poor in nickel and a sediment rich in it, as show in the table 3.11.

TABLE 3.11: XRF data of solution with not enough GLOVEL 800 A and its sediment.

Solution		Sediment	
Zn (g/l)	Ni (g/l)	%Ni	%Zn
12.4	0.9405	70	30

3.2 Cyclic voltammetry

Description of electrodes and machine parameters used for cyclic voltammetries are given in table 3.12. We choose a zinc piece as counter electrode to compensate zinc ion loss.

Start and stop potential are both 0 V, so that it's far enough from deposition beginning (about -1 V for zinc) and it's enough noble to assure total dissolution of deposit. We choose vertex potential equals to -1.7 V to study acidic bath additives ECOLUX STEEL A (paragraph 3.2.1.2) and ECOLUX STEEL C (paragraph 3.2.1.3). With alkaline (paragraph 3.2.2) solution cathodic structures shift to lower potential, so we change vertex potential to -2 V to assure complete deposition of all phases. Some preliminary tests at different scan rate show that at 50 mV/s peaks are more clear.

TABLE 3.12: Description of cell and scan parameters for cyclic voltammetries.

Cell definition		
Working	$1cm^2$ Steel sheet	
Counter	Zinc	
Reference	SCE	
Scan definition		
	Acidic bath	Alkaline bath
Initial Potential	0 V	0 V
Vertex Potential	-1,7 V	- 2 V
Final Potential	0 V	0 V
Scan rate	50 mV/s	50 mV/s

3.2.1 Acidic solution

Initial and final potential are 0 V, vertex potential is -1.7 V; optimal deposition parameters confirm this choice having good plating at -1.5 V.

3.2.1.1 Preliminary test

First cyclic voltammetries (figure 3.6), done to set the machine parameters, give some information about solution behaviour at low potential.

We analyse both solution without additive and complete ECOLUX STEEL^{TM}. We test two counter electrodes: a piece of zinc and a De Nora^{TM} metal mesh. Results are similar, first highlights peaks of solution without additives, second one those of ECOLUX STEEL^{TM}. Considering solution without additives (blue lines in the graph), there is an anodic peak at -0.35 V, indicating deposition of one phase, and a more broad cathodic peak at -0.25 V, stating dissolution of the previous deposit. Current is low, order of

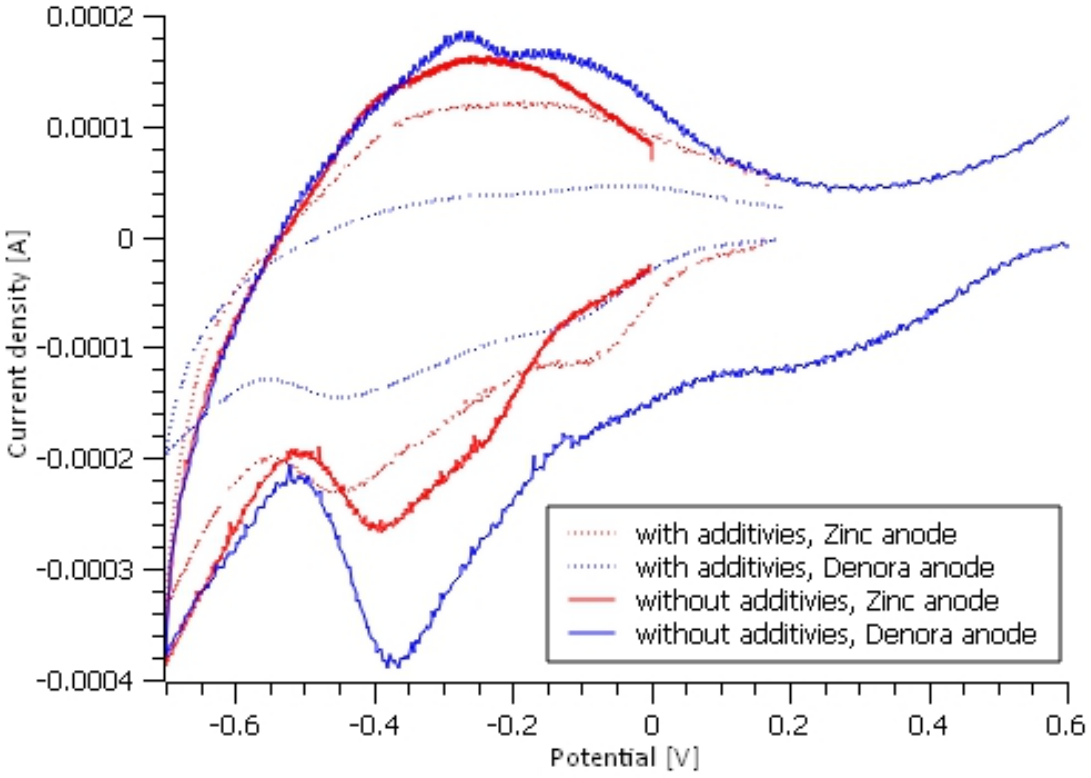

FIGURE 3.6: Cyclic voltammetries of acidic solution 0→-0.5V→0 with and without additives, using two types of counter electrode.

magnitude of 0.1 mA, so at this potential only deposition of secondary phases takes place. Additives have two main effects: current decreasing and shifting of the peaks to slightly more negative potential. We can assume that they are adsorbed on the cathode surface and form a barrier hindering and regulating transfer of ions from solution to substrate.

3.2.1.2 ECOLUX STEEL A

ECOLUX STEEL A work as levelling and grain-refining agent, it assure good deposition for a broad range of potential. To study its effect on the bath we start with solution without additives and vary its concentration from 0 to 15 ml/l, the optimal value (figure 3.7).

In the first step from 0 to -1.7 V there are changes in structures both in positive and in negative current. Without additive current decreases linearly reaching 0 at -0.55V.

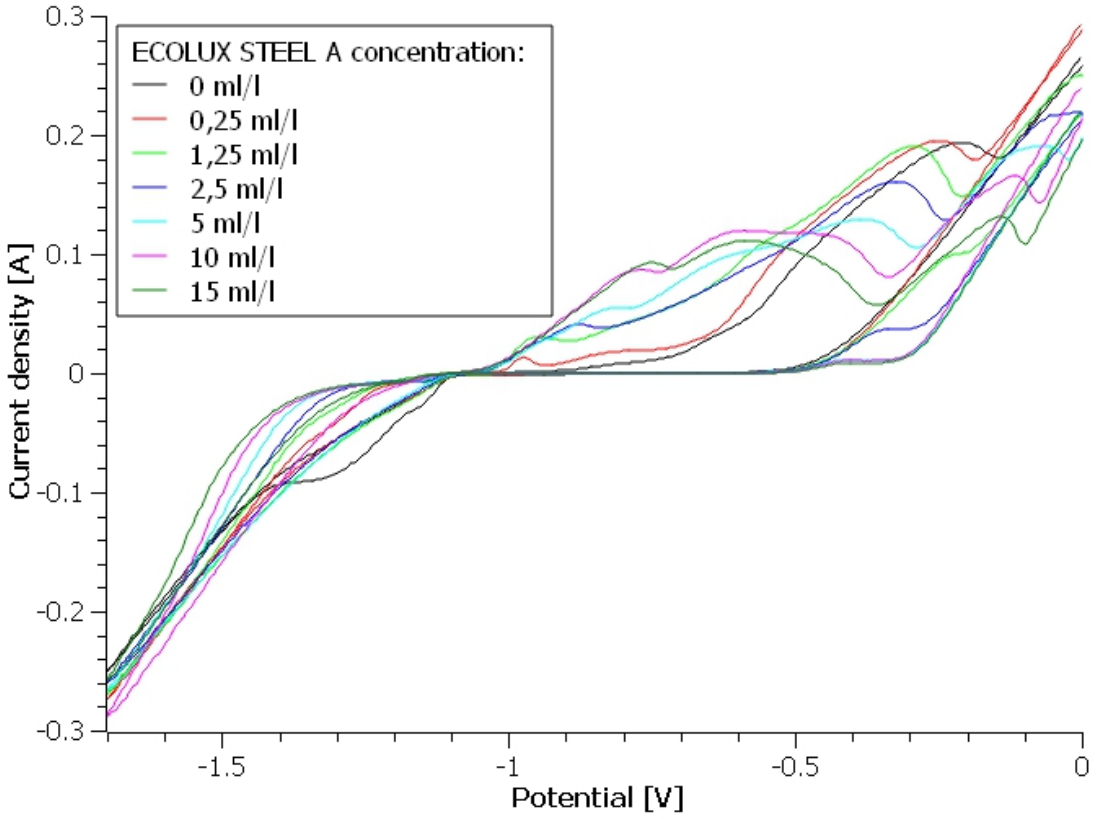

FIGURE 3.7: Cyclic voltammetries of acidic solution 0→-1.7V→0 varying ECOLUX STEEL A concentration.

Increasing additive concentration, current decreases and it creates a little step stabilized at -0.4 V over 5 ml/l. We can assume that it is a consequence of additive adsorption on surface: it create a barrier against current flow, to overcome it we have to applying a potential higher than -0.3 V.

Cathodic branch without additive presents a hump at about -1.15 V and a peak at -1.3 V. Adding ECOLUX STEEL A these structures disappear and it forms a step at the beginning of the deposition, about -1.1 V. Increasing the concentration it extends till -1.3 V with 15 ml/l. Current remains low, about 0.01 A, so we can assume that it's the barrier effect of surface adsorbed additive.

After potential inversion current decreases linearly to zero. In the anodic branch, structure is more complex. Without additive dissolution starts at about -1V, then there are two humps, first one at -0.65 V and second one at -0.5 V, and a peak at -0.2 V. Adding ECOLUX STEEL A a new peak is formed at about -0.95 V, then increasing

concentration it becomes more intense and nobler. All the other structures shift to lower potential. First hump (-0.75 V) joins the new peak; the second one (-0.6 V) becomes more intense, the peak (-0.45) lowers instead. Above 1.25 ml/l a new structure appear at high potential, forming a peak at -0.15 V.

ECOLUX STEEL A strongly affects electrochemical behaviuor of the acidic solution. Anodic structures at lower potential can be assigned to dissolution of the zinc in the alloys; considering XRD results, it is mainly γ phase. The peak at -0.15 V indicates dissolution of the remaining nickel. As XRD suggests, phase type doesn't change, deposit remains substantially monophasic γ. But observing SEM image of surface, we can assume that this additive controls grain structure causing change in voltammetry signal.

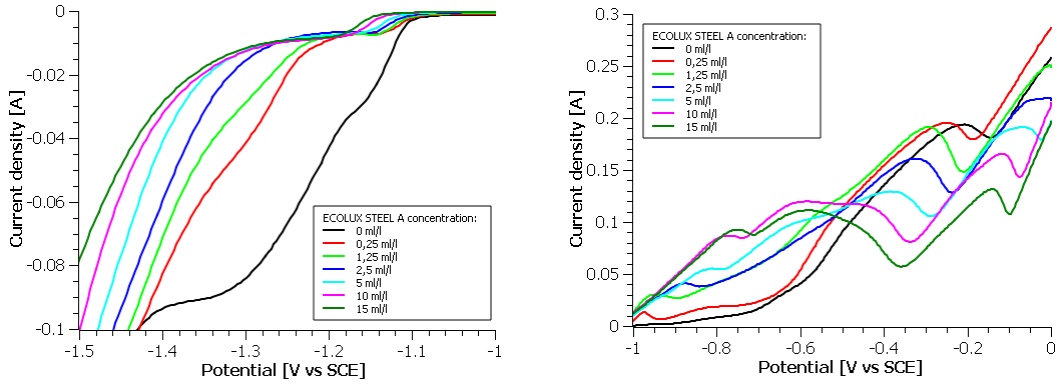

(a) Cathodic peaks

(b) Anodic peaks

FIGURE 3.8: Magnifications of voltammetry peaks varying ECOLUX STEEL A concentration.

3.2.1.3 ECOLUX STEEL C

ECOLUX STEEL C works as complexing agent, it maintains metal ions in solution and it controls their deposition assuring layer brightness and bath clearness. To study its effect on the bath we start with no additive solution and vary its concentration from 0 to 15 ml/l, the optimal value (figure 3.9).

In the cathodic branch, increasing additive concentration the peak at -1.3 V disapppears and the curve assumes a linear trend. Cathodic current increases indicating greater deposition. Absence of peaks indicates that hydrogen evolution takes place at the same time of deposition.

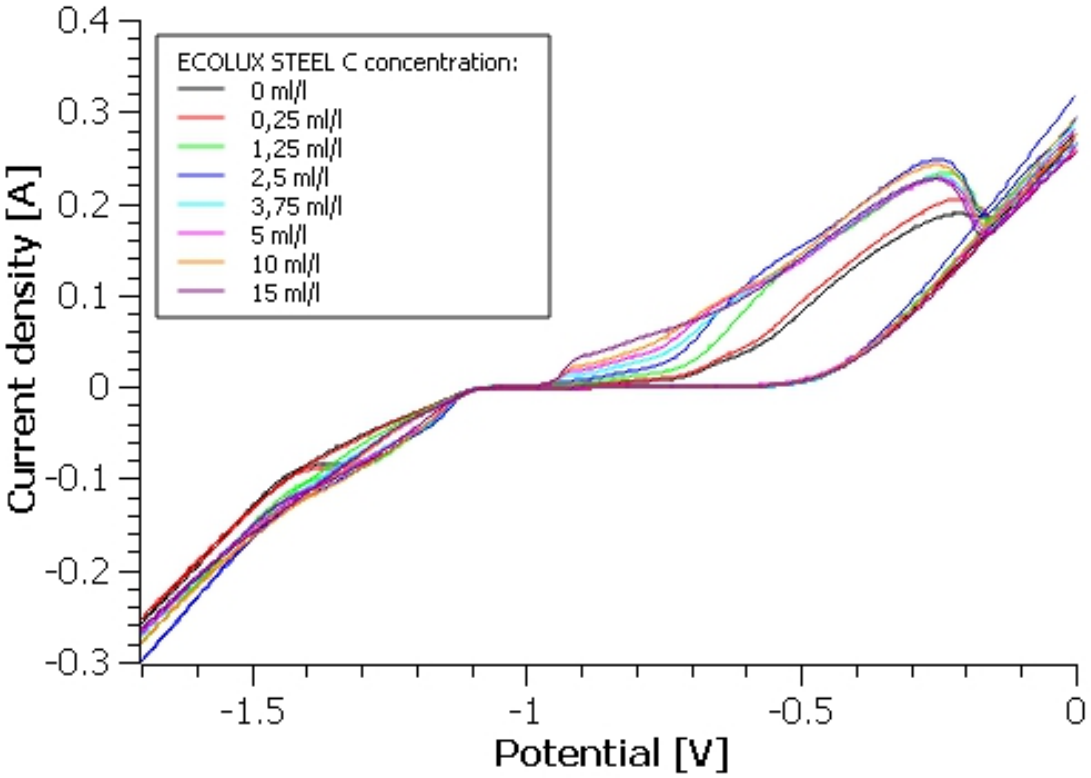

FIGURE 3.9: Cyclic voltammetries of acidic solution 0→-1.7V→0 varying ECOLUX STEEL C concentration.

Structures in the anodic branch tend to be defined increasing ECOLUX STEEL C. It forms a step at the beginning of dissolution, about -0.95V. Peak at -0.2 V shifts to -0.25 V, becomes more narrow and higher. With optimal additive concentration all the anodic curve is shifts to higher current, e.g. peak goes from 2 A to 2.6 A.

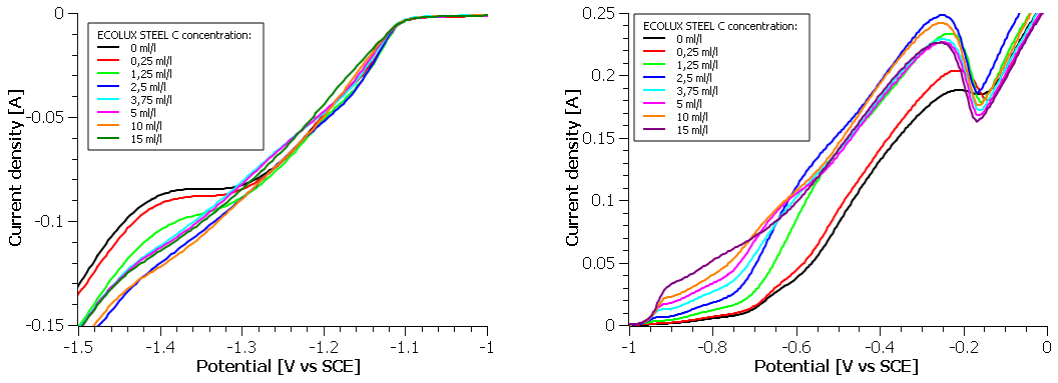

(a) Cathodic peaks

(b) Anodic peaks

FIGURE 3.10: Magnifications of voltammetry peaks varying ECOLUX STEEL C concentration.

With ECOLUX STEEL C bath deposits a greater amount of alloy with a more defined phase, with higher resistance against corrosion. [26] [22] [53] [27] [63] [65]

3.2.1.4 Deposition with single additive baths

To investigate further the effect of each additive we do deposition test with solution containing only one additive. We have two solutions based on bath B: BA contains 15 ml/l of ECOLUX STEEL A, BC contains 15 ml/l of ECOLUX STEEL C. Parameters chosen for galvanostatic are the same used for solution B without additives. Table 3.13 shows properties of relative samples.

TABLE 3.13: Samples obtained with single additive solutions.

Sample	Deposition parameters		XRF data		
	Current (mA/cm^2)	Time (min)	Thickness (μm)	%Ni	%Zn
BA1	35	13	7,4	0,76	99,24
BC1	35	13	11,4	16,8	83,2

First solution is cloudy, it suffers ion instability consequently composition isn't right; too low nickel content of sample BA1 indicates depletion of this metal in the bath maybe due to lack of ECOLUX STEEL C.

Second solution is more limpid, its aspect is similar to ECOLUX STEEL^{TM}. Sample BC1 shows properties very similar to samples obtained with B solution, only a little richer in nickel.

3.2.2 Alkaline solution

Initial and final potential are 0 V as acidic solution, we lower vertex potential to -2 V; optimal deposition parameters confirm this choice: having good plating at -1.6 V, we can assume that at -2 V bath deposits all possible phases.

By some preliminary deposition tests, we find that GLOVEL 800 A and Complex Ni are essential for bath stability, without them nickel ions can't deposit and a sediment appears. In fact Complex Ni is the source of nickel ions and it must be premixed with

GLOVEL 800 A to assure ion stability in bath. Therefore we study only Additivo Ni b.d.c.

To observe the effects of this additve we do 8 cyclic voltammetries varying its concentration from 0 to 6 ml/l (figure 3.11).

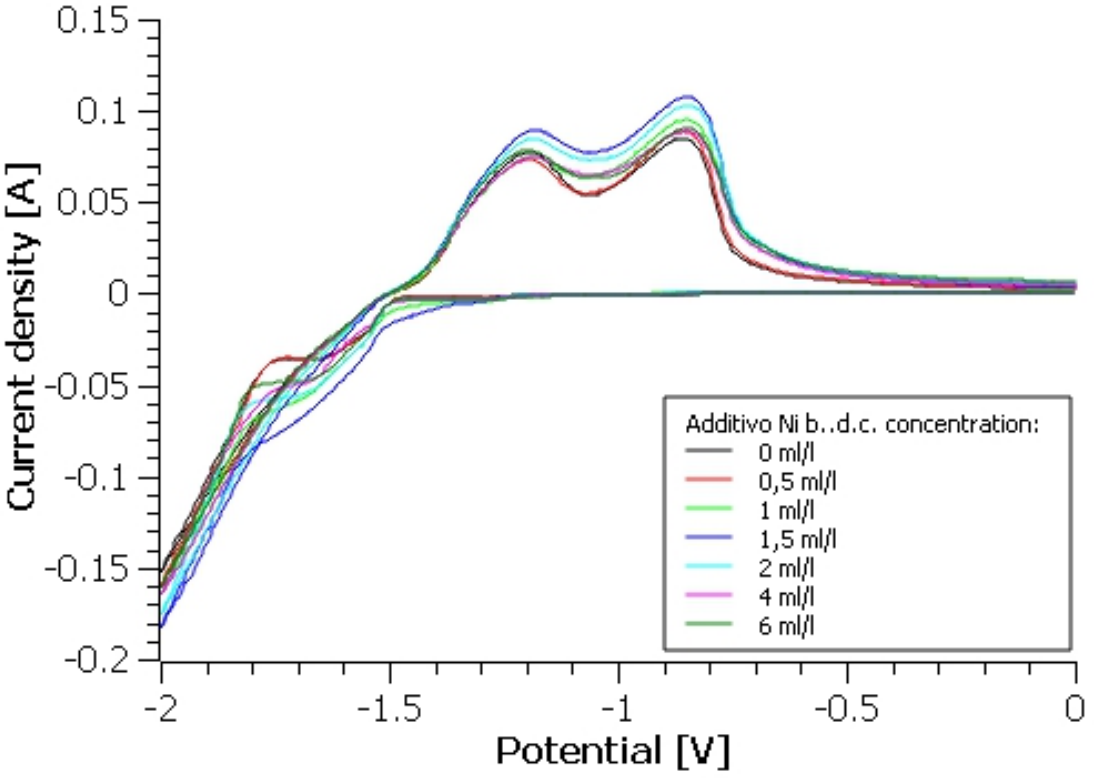

FIGURE 3.11: Cyclic voltammetries of acidic solution 0→-2V→0 varying Additivo Ni b.d.c. concentration.

In the cathodic branch there are two interesting structures: a hump at about -1.55 V and a peak at -1.7 V, they indicate two deposition process.

Anodic branch confirms this thesis: there are two distinct peak, first at -1.2 V and second at -0.85 V; we can assume that they indicate dissolution of zinc and nickel in the γ phase.

Increasing additive concentration, current increases slightly till 15 ml/l, then it returns to initial values; variations are low, about 0.2 A. So Additivo Ni b.d.c. doesn't influence very much electrochemical behaviour of the bath, without changing type and amount of phases.

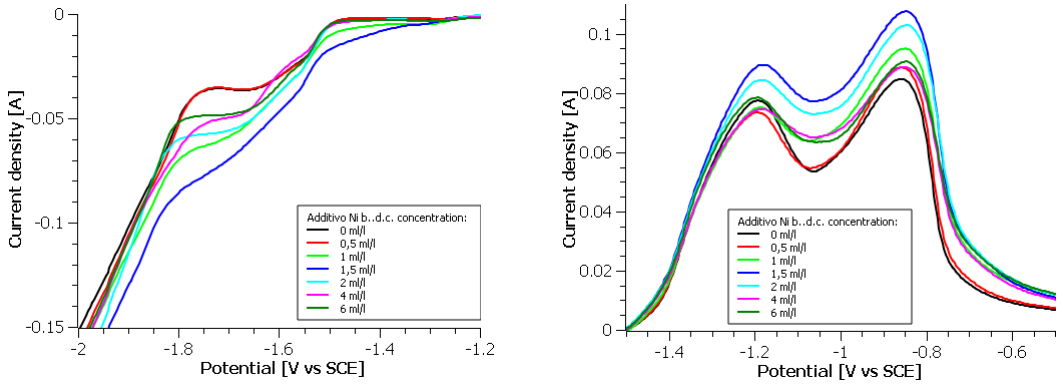

(a) Cathodic peaks

(b) Anodic peaks

FIGURE 3.12: Magnifications of voltammetry peaks varying Additivo Ni b.d.c. concentration.

3.3 XRD

XRD allows structure analysis of the samples, detecting phases and crystal orientation of the plated layer. Table 3.14 summarises analysed samples with their properties. We are interested in comparing layer plated with different baths to understand effect of additives in acidic bath and difference between acidic and alkaline solution. [44] [9]

TABLE 3.14: XRD samples.

Sample	Deposition parameters			XRF data		
	Potential (V vs SCE)	Current density (mA/cm^2)	Time (min)	Thickness (μm)	%Ni	%Zn
A31	-2.45		1.5	6.59	12.4	87.6
A33		240	1.5	7.35	12.4	87.6
A36		25	21	10	13.1	86.9
A37		25	21	10.9	12.4	87.6
B13		80	5	10.9	13.8	86.2
B14		90	4.5	10.9	13.9	86.1
C10	-1.6		120	11.4	13.2	86.8
D1	-1.6		110	8.93	14.5	85.5

- A31

  Pattern of sample A31 has many of the typical γ phase peaks. Most significant are at 43°, 78.7° and 35°. In particular, the first relating to crystallographic planes (330) and (411) is much higher than the last indicating preferential orientation of crystals.

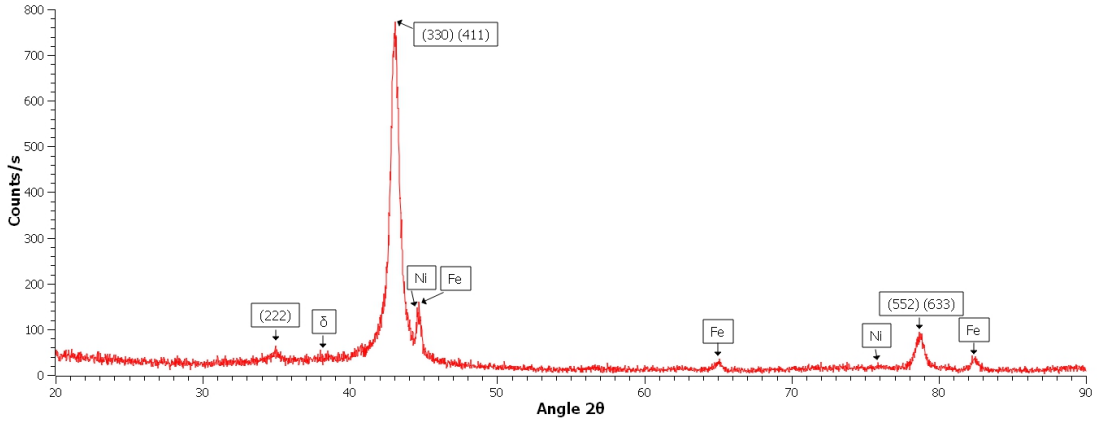

FIGURE 3.13: XRD pattern of sample A31.

Substrate causes peaks at 44.7°, 65° and 82.2° related to iron. There are also small traces of nickel signal at 44.5° and 76.3°. Structures around 38° indicate presence of δ zinc nickel phase.

- A33

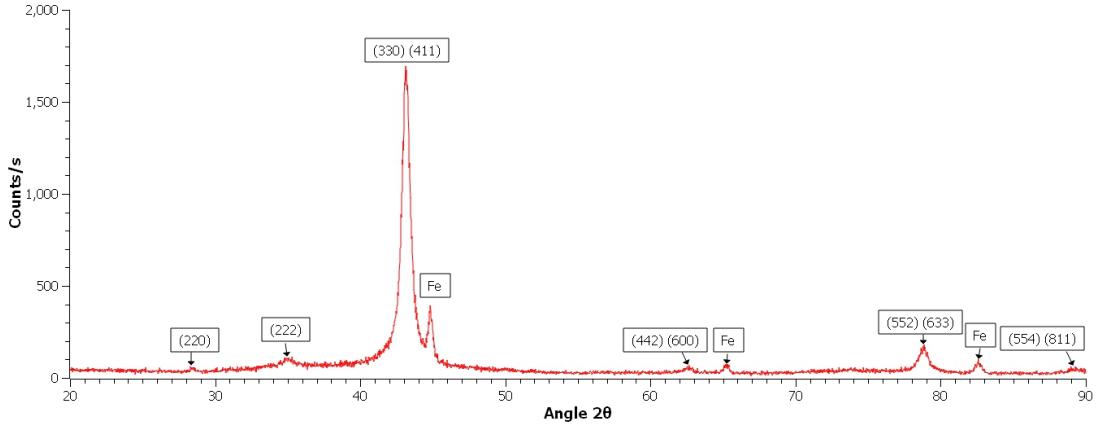

FIGURE 3.14: XRD pattern of sample A33.

Pattern of sample A33 presents almost the same peaks of A31 one; this reflects similar deposition parameters and confirms XRF data. All the peaks are higher than those of sample obtained in potential control are, so we can assume more defined phase structure thanks to current control.

As previous sample, highest signal is at 43°, relating to crystallographic planes (330) and (411). Other peaks are low, so crystals maintain same preferential orientation.

Other little γ peaks appear: at 28° (220), at 62.1° (442) (600) and at 89.2° (554) (811).

There are typical iron peaks at 44.7°, 65° and 82.2°, minor traces of nickel, zinc and δ phase.

- A36

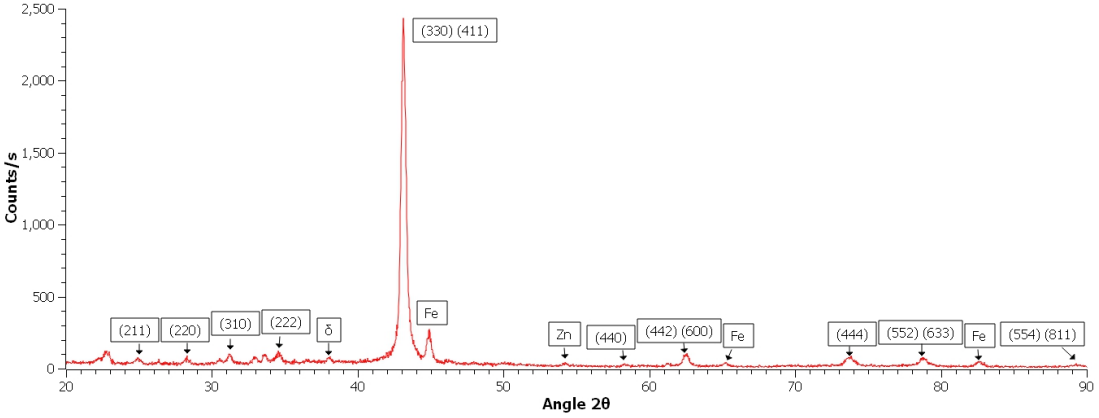

FIGURE 3.15: XRD pattern of sample A36.

In pattern of sample A36 there are many structures, most of them relating to γ phase peaks. Peak at 43° becomes even more predominant, so crystals grow preferentially along planes (330) and (411). Other visible γ peaks are at 24.8° (211), 28° (220), 31.5° (310), 34.5° (222), 58.5° (440), 62.1° (442) (600), 73.1° (444), 78.7° (552) (633) and 89.2° (554) (811).

Low deposition current promote codeposition of solution by-products: small peak at 38° and 54.2° state respectively δ zinc nickel and metal zinc.

We can find iron peaks relating to substrate at 44.7°, 65° and 82.2°.

- A37

Pattern of sample A37 is very similar to sample A36 one. The main differences are two: higher intensity of the peaks, in particular 43° one, and decreasing of structures from 25° to 35°. We can assume a more defined phase structure of the layer due to single step deposition, instead sample A36 is obtained in multi-step process.

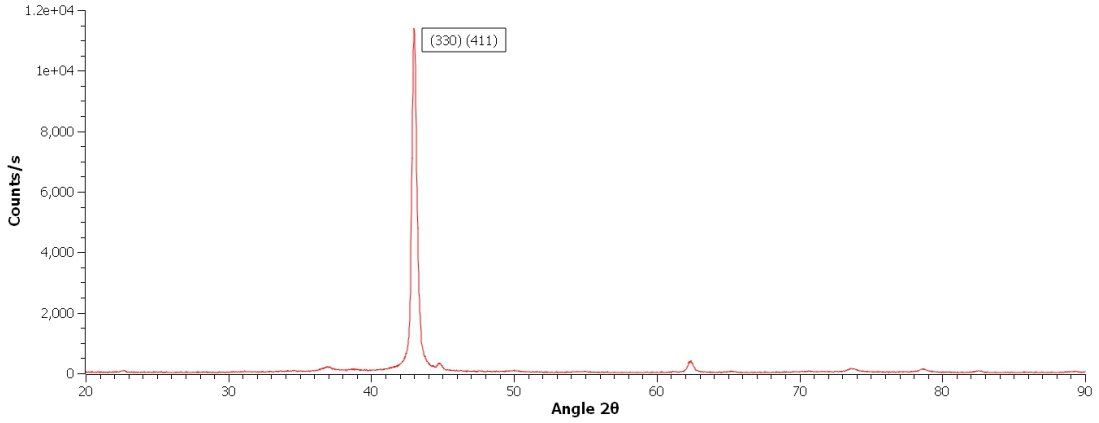

(a) Complete XRD pattern.

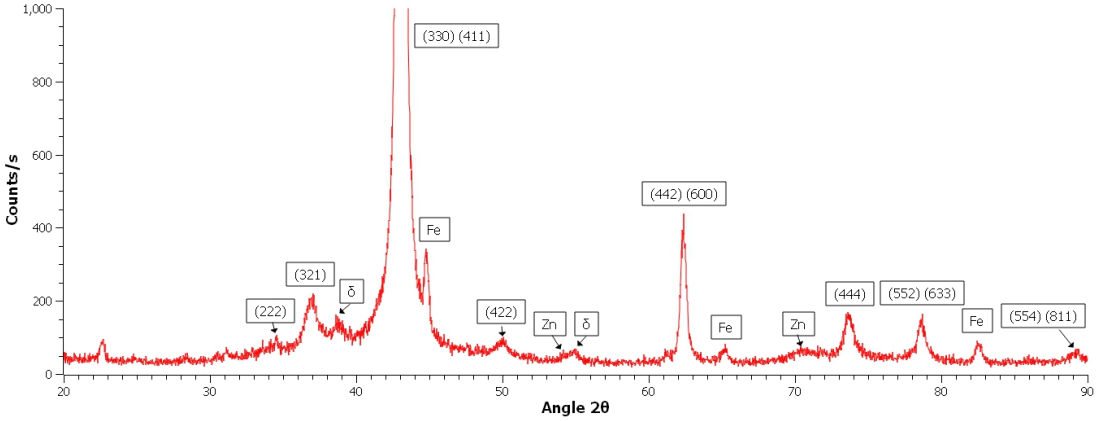

(b) Magnification of low intensity peak.

FIGURE 3.16: XRD pattern of sample A37.

In addition to 43° peak, other significant γ phase peaks are at 34.5° (222), 37.4° (321), 49.9° (422), 62.1° (442) (600), 73.1° (444), 78.7° (552) (633), 89.2° (554) (811).

There are small amounts of δ phase, indicated by peaks at 38° and 55°, and traces of zinc, peaks at 54.2° and 70.7°.

Iron substrate is responsible of peaks at 44.7°, 65° and 82.2°.

Deposition conditions used for this sample are optimal ones: intensity of the peaks indicate that it's almost only zinc nickel γ phase, assuring best corrosion resistance.

- B13

  Pattern of sample B13 contains almost only γ phase peaks: that at 43° is the highest so grains are oriented as the previous samples; other significant peaks are

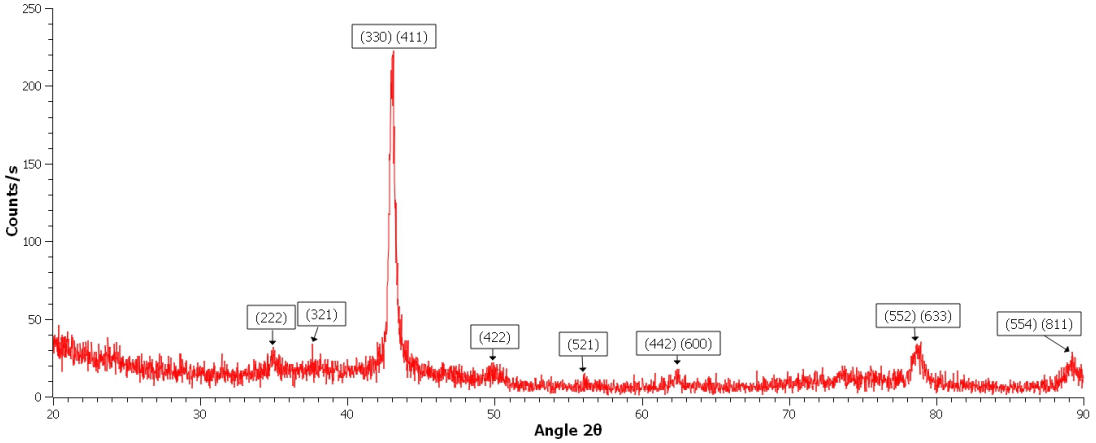

FIGURE 3.17: XRD pattern of sample B13.

at 35° (222), 37.4° (321), 49.9° (422), 56° (521), 62.1° (442) (600), 78.7° (552) (633), 89.2° (554) (811).

There are traces of zinc and iron.

Intensity of signal is much lower than previous samples, so we can assume that without additives bath works badly and the deposit contains less γ phases.

- B14

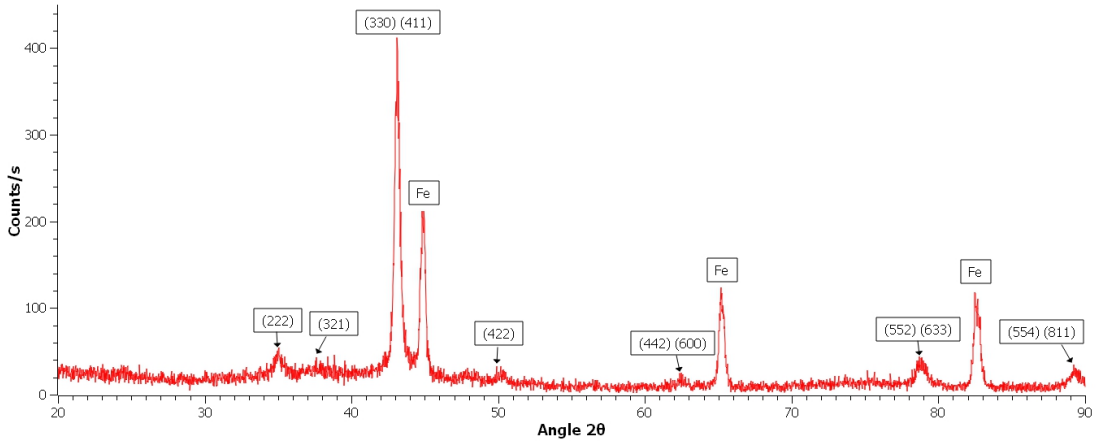

FIGURE 3.18: XRD pattern of sample B14.

Pattern of B14 is very similar to the B13 one; in fact, deposition parameters look alike. There are two differences: the typical iron substrate peaks (44.7°, 65° and 82.2°) appear and intensity of all structures is higher, indicating a more defined phase structure.

- C10

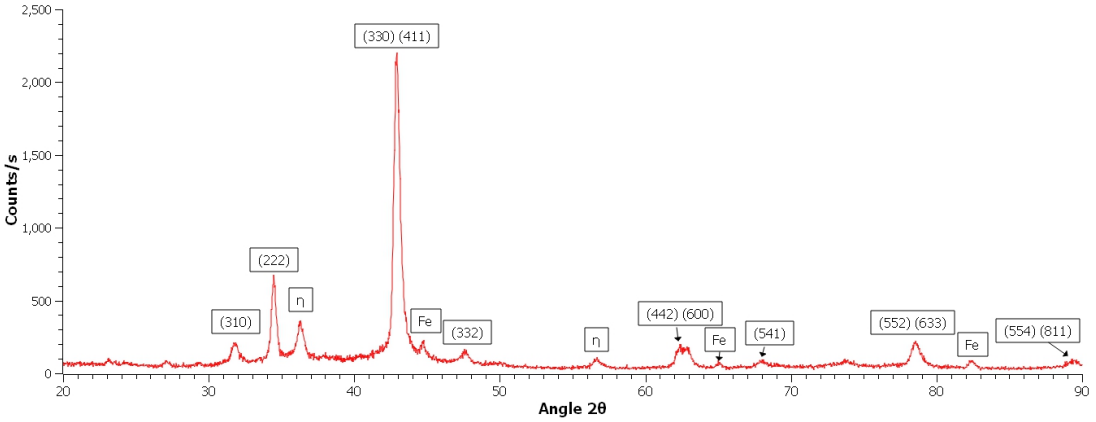

FIGURE 3.19: XRD pattern of sample C10.

Pattern of sample C10 contains many peaks of zinc nickel γ phase. The highest one is at 43° relating to planes (330) (411). Other significant peaks are at 31.5° (310), 34.5° (222), 47.6° (332), 62.1° (442) (600), 68° (541), 78.7° (552) (633), 89.2° (554) (811).

There are little peaks of iron substrate at 44.7°, 65° and 82.2°.

Peaks at 36.4° and 56.7° can be assigned to small amounts of η zinc nickel.

- D1

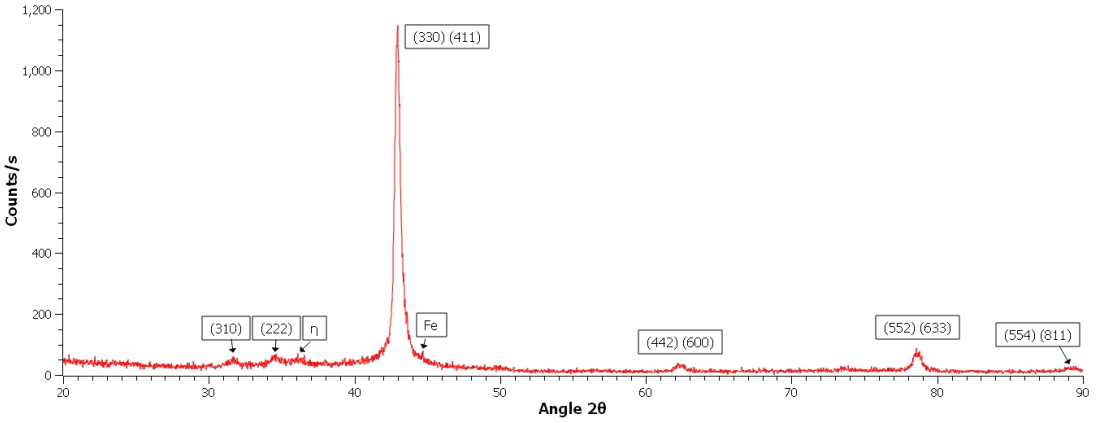

FIGURE 3.20: XRD pattern of sample D1.

Pattern of sample D1 contains few peaks, all relative to zinc nickel γ phase. The highest is at 43° relative to planes (330) and (411), little ones are at 31.5° (310), 34.5° (222), 62.1° (442) (600), 78.7° (552) (633), 89.2° (554) (811).

There are traces of iron substrate at 44.7°, of η phase at 36.1° both very low.

Intensity is about half of sample C10 one, so we can assume a less defined structure in the layer. [44] [53]

3.4 GDOES

GDOES analysis allows study of elemental content along the depth of the layer, so we can evaluate composition distribution. Thanks to high sensitivity, it can detect hydrogen entrapped into the deposit and the substrate. It's interesting to examine possible hydrogen distribution changes due to bath additives.

Sample surface must be flat because system has to create vacuum around examined area. After test of same samples to calibrate the machine, we analyse samples A48 and B31 (in table 3.15 relative deposition information). Figure 3.21 compares depth profile of the most interesting element. The quantity on y axis is the relative intensity, we don't have enough data to correlate it with element quantity. So we can only compare signals of same same element in different samples but not signals of different elements.

TABLE 3.15: GDOES samples

Sample	Deposition parameters		XRF data		
	Current density (mA/cm^2)	Time (min)	Thickness (µm)	%Ni	%Zn
A48	25	25	11.7	15.3	84.7
B31	35	13	10.0	15.7	84.3

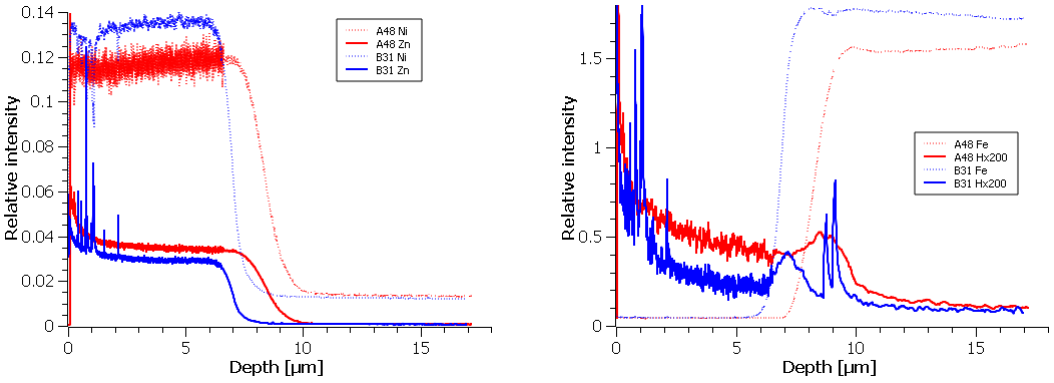

(a) Ni (dotted line) and Zn (solid line)

(b) H (solid line) and Fe (dotted line)

FIGURE 3.21: GDOES results: comparison between samples A48 (red line) and B31 (blue line).

GDOES analysis confirms XRF data: deposited metal signals of sample A48 fall down about 2 μm after the corresponding signals of sample B31, in fact thickness difference measured by XRF is 1.7 μm. Furthermore nickel content in sample A48 is higher than in sample B31 and consequently zinc content in sample A48 is lower than in sample B31 in agreement with XRF.

Both zinc and nickel signals are almost constant. First has a substantial increase near the external surface. Instead second a slight gradual reduction from the inner to outer side, this is in agreement with deposition test that show a decrease in nickel content with increasing deposition time.

Signal of sample B31 presents noise near the surface, indicating possible defect in the layer. A48 shows a more gradual change between plated layer and iron substrate.

The signal trend of hydrogen is the same for both the samples: it's higher near the external surface, then decreases due to diffusion process into the layer; at the substrate interface there is a broad peak and finally signal goes to almost zero into steel piece. Main difference is in the interface layer-substrate: in sample B31 hydrogen increases significantly, instead in sample A48 the peak is slightly higher than the signal in the layer. We can assume that additives reduce hydrogen diffusion into the substrate, decreasing its negative effects on steel. [38] [57]

3.5 SEM

The aim of this analysis is observation of the surface morphology and grain structure of the deposit, both along the section and on outer side. In particular we want to find the differences between deposits from bath with additives and those from bath without additives.

We prepare two samples, A46 and B29, by deposition with EG&G system. Table 3.16 shows the parameters, chosen to have right composition and thickness, and XRF results.

Each sample is cut in half by means scissors. One is used for morphology observation, so it is put into the microscopy as is. Other one for the study of section is embedded into resin disk and fixed into the right position. Then we polish the surface by means polishing paper (120, 320, 600, 1200, 4000) and 1μm paste to expose flat surface. In

TABLE 3.16: SEM samples

Sample	Deposition parameters		XRF data		
	Current density (mA/cm^2)	Time (min)	Thickness (μm)	%Ni	%Zn
A46	25	25	10.7	15.7	84.3
B29	35	12	8.96	15.4	84.6

the end 20 second acid attack with nital 1 highlights grains by selective corrosion of the borders. [25] [36]

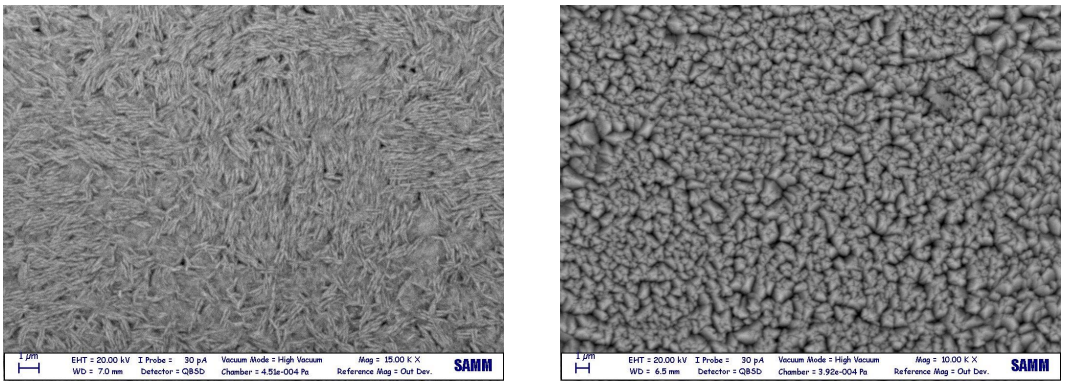

(a) A46 (b) B29

FIGURE 3.22: A46 and B29 morphology SEM figures.

As we can see from the pictures, additives have great influence on the morphology. A46 grains have elongated shape, with a good compact distribution, in fact there are few voids on the surface. Instead B29 sample shows micrometric structures like peaks separated by deep valleys.

The particular shape of the structure in the first sample can be explained by the effect of the grain-refiner agent that can control the growth, in this case with preferred growth direction. Higher compactness and flatness of the surface it's a good effect of the additives, in fact reduction of the roughness increases corrosion resistance.

B29 section picture shows plated layer with many cracks. Larger ones are along the growth direction, some of those reach external surface creating the voids that characterize the morphology. Thinner cracks parallel with surface start from previous ones, in some case connecting two or more of them. [19]

As indicated by the scale, layer thickness is about 8 μm; composition diagram in figure 3.24 shows high Zn-Ni signal with 8μm extension confirming this measure. The value is

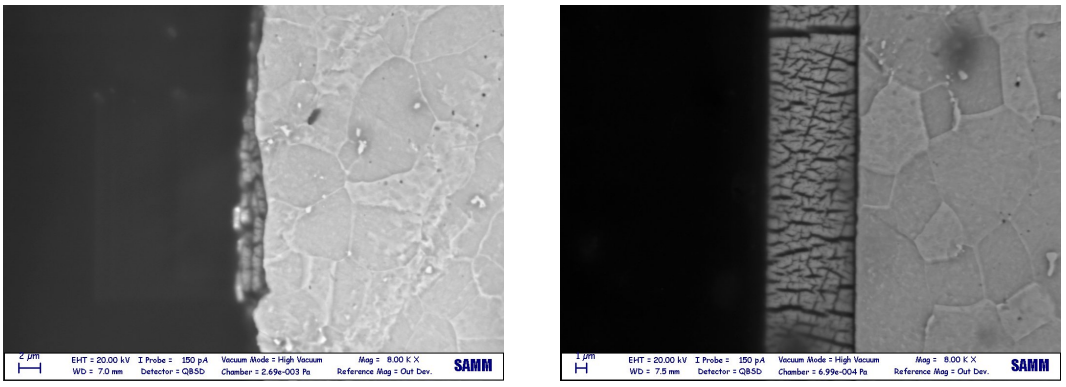

(a) A46 (b) B29

FIGURE 3.23: A46 and B29 section SEM figures.

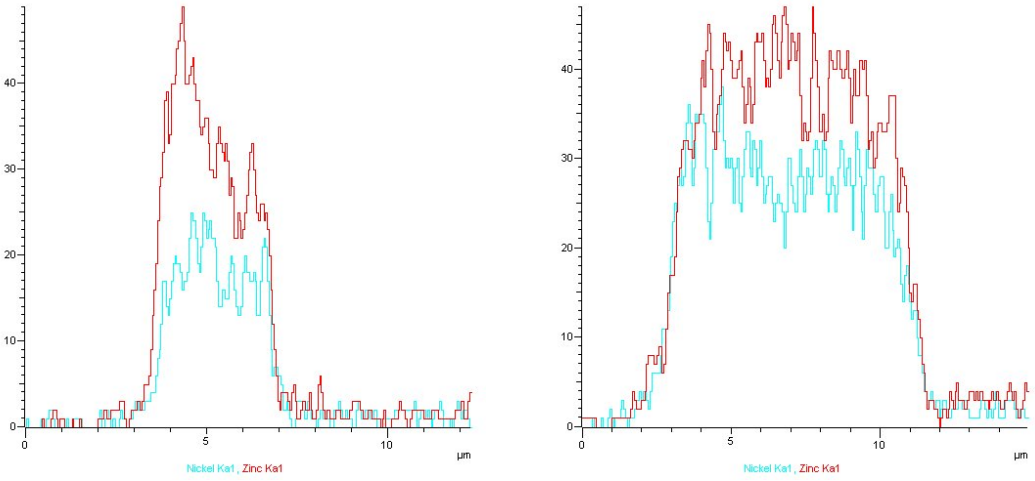

(a) A46 (b) B29

FIGURE 3.24: Content of nickel (blue line) and zinc (red line) in samples A46 and B29 by SEM analysis.

also close to XRF data (8.96µm). The composition is rather uniform along the depth. [49]

A46 section suffers same damage due to polishing, it's peeled off in same points and layer is too thin. We can recognise cracks similar to sample B.

3.6 Characterization of fasteners plated with acidic zinc nickel

3.6.1 Potentiodynamic polarization

Potentiodynamic polarization allow us to evaluate corrosion behaviour of the plated layer, in particular we want to compare through corrosion potential and current the resistance of different post-plating finishings.

Samples for this analysis are 4 bolts plated with ECOLUX STEEL ^{TM}, each with a different surface finishing:

- as plated with ECOLUX STEEL^{TM}
- passivated
- heat treated for dehydrogenation
- passivated and heat treated for dehydrogenation

Chromium conversion film is usually applied on zinc coating as physical barrier increasing corrosion resistance; in our case it's a blue bright type. Heat treatment for dehydrogenation can change zinc-nickel phase and can degrade passivated layer.

We use a three electrodes configuration cell: bolt is the working electrode, platinum wire is counter electrode and SCE is the reference electrode. The electrodes are immersed in 35 g/l sodium chloride solution.

EG&G controls all electrodes. We apply a linear sweep voltammetry from -0,1 V vs OCP to 1,5 V and 1 mV/s as scan rate. Results are shown in table 3.17.

Table 3.17: Corrosion potential and current from potentiodynamic analysis.

Finishing	Corrosion potential (mV vs SCE)	Corrosion current density ($\mu A/cm^2$)
As plated	-934	90
Passivated	-949	39
Heat treated	-751	51
Passivated and heat treated	-724	25

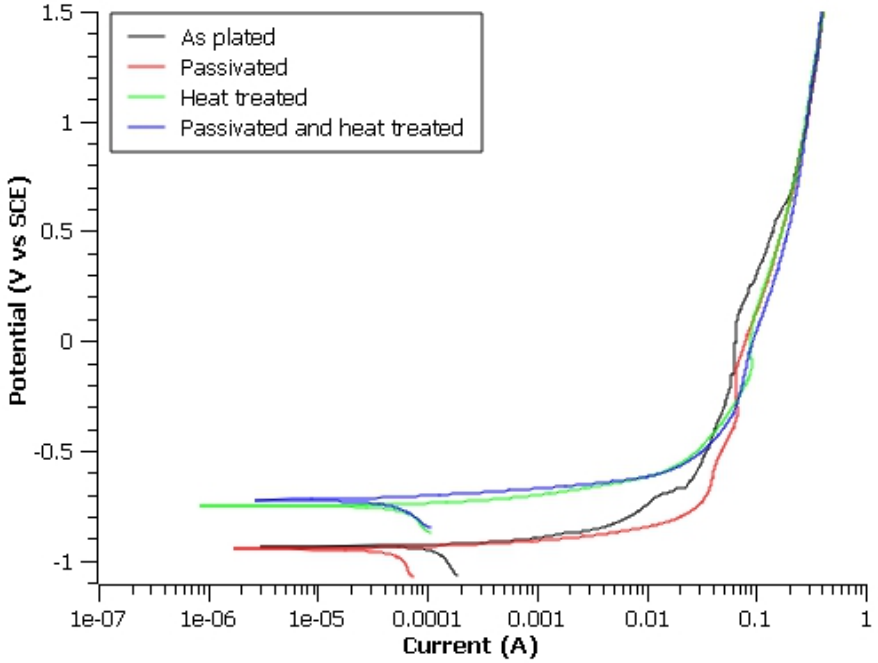

(a) Complete potentiodynamic plot

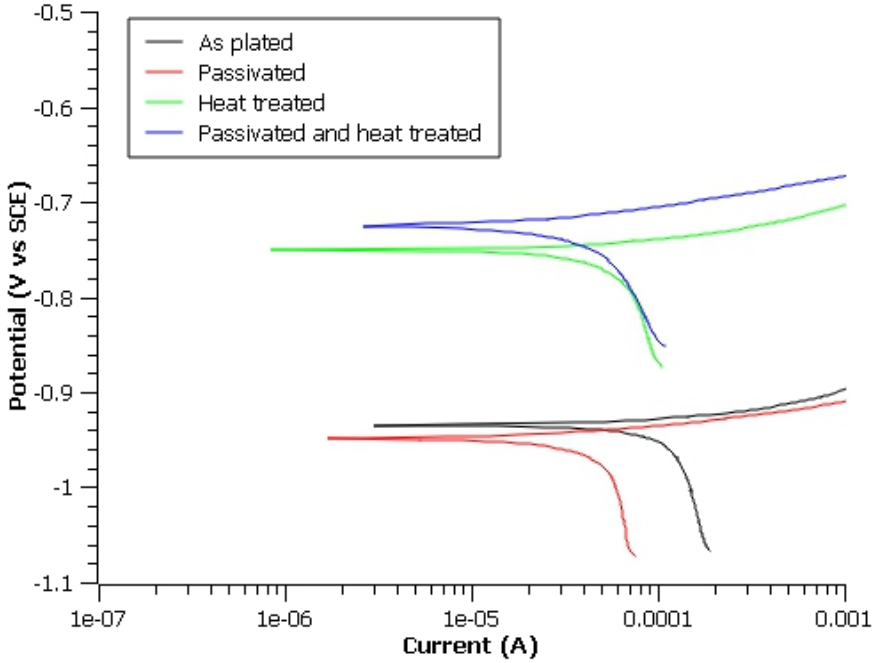

(b) Magnification of the peak zone

FIGURE 3.25: Potentiodynamic polarization potential-logarithmic current density graph with magnification of the peak zone.

Analysis of the curves in figure 3.25 by Tafel fitting method allows us to calculate corrosion potentials and currents collected in table 3.17. Potential values are in the typical range of zinc-nickel plated layer: a little nobler than zinc (-1000 mV), due to nickel content, but below below steel value (-600 mV) to assure cathodic protection of the substrate. [15] [16]

Potential is strongly influenced by heat treatment: corrosion potential increases by about 220 mV with passivation and 180 mV without. This improvement in nobility can be explained by phase and structure change due to thermal treatment that ensure stronger barrier against corrosion.

Passivation clearly influences corrosion rate: it reduces by about 50% corrosion current density slowing down degradation process. This analysis suggests that after passivation and heat treatment layer work better against corrosion, assuring higher nobility and lower corrosion rate. [32] [26] [27] [3] [59]

3.6.2 XRD

We analyse bolts (table 3.18) used in potentiodynamic polarization to observe effect of passivation and heat treatment on phase structure.

Table 3.18: Treatment of bolts analysed with XRD.

Surface finishing
As plated
Passivated
Heat-treated
Passivated and heat-treated

- As plated

  Plated bolt pattern contains some zinc nickel γ phase peaks, as previous samples. The main difference is that the highest intensity is at 62.1°, relating to crystal plane (442) (600). This indicates a change of the grain preferential orientation. The 43° peak becomes the second most intense; other significant peak are at 34.5° (222), 49.9° (422), 78.7° (552) (633), 89.2° (554) (811). There are iron substrate peaks at 44.7°, 65° and 82.2°.

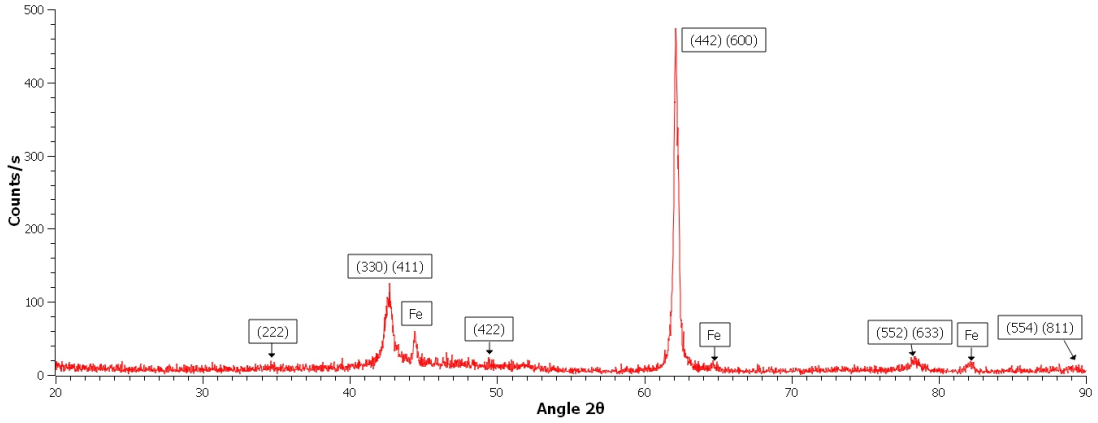

FIGURE 3.26: XRD pattern of plated bolt.

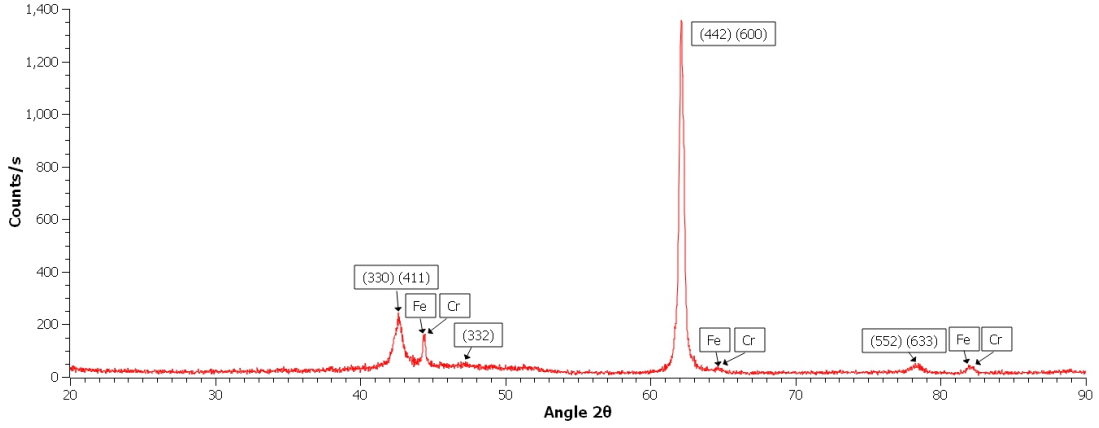

FIGURE 3.27: XRD pattern of passivated bolt.

- Passivated

  Passivated bolt pattern is similar to previous one: 62.1° peak is the highest among γ phase, other are at 43°, 47.6°, 52°, 78.7°. There are two differences: chromium and iron peaks appear and intensity of all structures is higher, indicating a more defined phase structure.

- Heat-treated

  Heat treatment affect very much XRD pattern: compared to plated bolt, many zinc nickel γ phase peaks compare and their intensities change. Peak at 43° relating to planes (330) and (411) becomes the highest, at the expense of 62.1° one. Other significant peaks are at 31.5° (310), 34.5° (222), 37.4° (321), 47.6° (332), 49.9° (422),

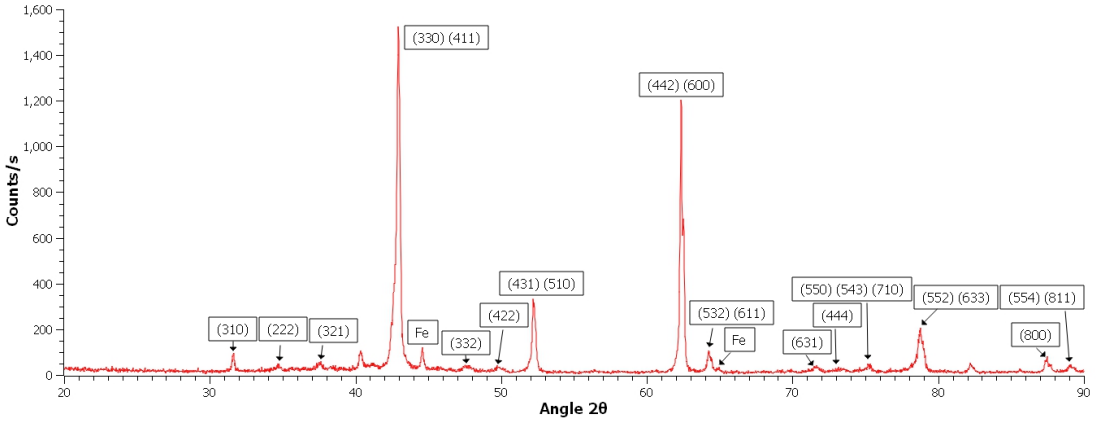

FIGURE 3.28: XRD pattern of heat-treated bolt.

52° (431) (510), 64° (532) (611), 71.6° (631), 73.1° (444), 75.5° (550) (543) (711), 78.7° (552) (633), 87.5° (800), 89.2° (554) (811).

We can assume that heat treatment causes reorganisation of the crystals with orientation change.

There are iron substrate peaks at 44.7° and 82.2°.

- Passivated and heat-treated

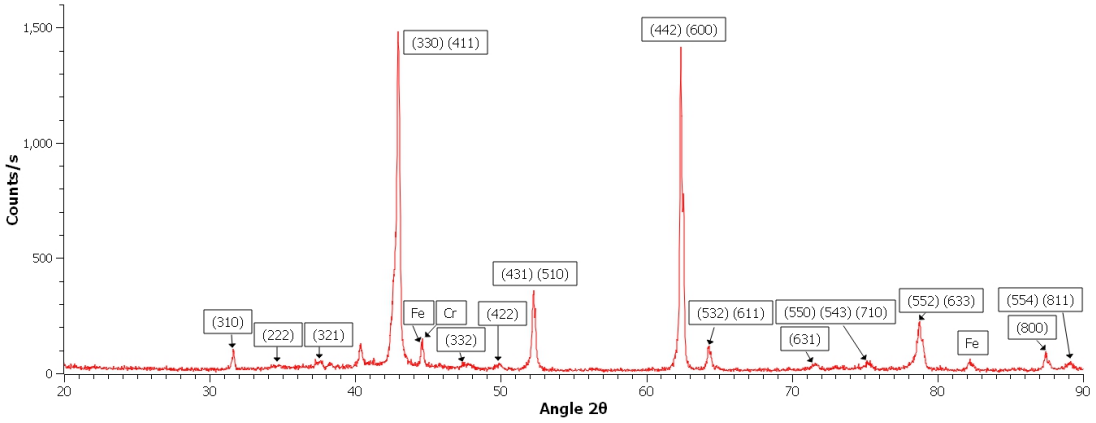

FIGURE 3.29: XRD pattern of passivated and heat-treated bolt.

Pattern of passivate and heat-treated bolt is very similar to previous one. At 43° and 62.1° we have maximum of intensity, so gamma phase crystals are oriented along relative planes, but there are many other peaks of this phase less intense.

Iron and chromium peaks are visible at 44.7°, 65° and 82.2°.

3.6.3 GDOES

We analyse three plated bolts obtained with different process:

- Zinc plating
- Acidic zinc nickel plating (ECOLUX STEEL^{TM})
- Acidic zinc nickel plating (ECOLUX STEEL^{TM}) followed by thermal treatment for dehydrogenation.

Figure 3.30 shows hydrogen, zinc, nickel and iron depth profile of the bolts. We have a particular interest in possible variation of the hydrogen diffusion into the layer and the substrate.

All the plated layer are about 7-9 µm thick, common values for this type of corrosion protection coating.

In the first bolt, zinc intensity increases going deeper and the transition at substrate interface is gradual. In second bolt, nickel and zinc signal are constant along the thickness, assuring phase homogeneity in the layer; transition at substrate interface is more rapid. In third bolt, zinc and nickel signals slightly increase going deeper, due to metal diffusion during thermal treatment; transition remains rapid has previous bolt.

In zinc plated fastener, hydrogen profile is constant in the coating and slightly decreases at the substrate interface continuing in the steel. Therefore hydrogen species are present also in the substrate at the interface with the coating.

In acidic zinc nickel coated fastener, hydrogen profile decreases in the first 3 micrometers of the coating then decline slowly continues. So it does not show any evidence of embrittlement of the substrate.

The hydrogen profile does not change significantly after thermal treatment, signal decrease is slightly more rapid only. It suggests that ECOLUX STEEL^{TM} effectively minimizes hydrogen content, making thermal treatment effect insignificant.

We can conclude that ECOLUX STEEL^{TM} reduces hydrogen content avoiding harmful embrittlement effects.

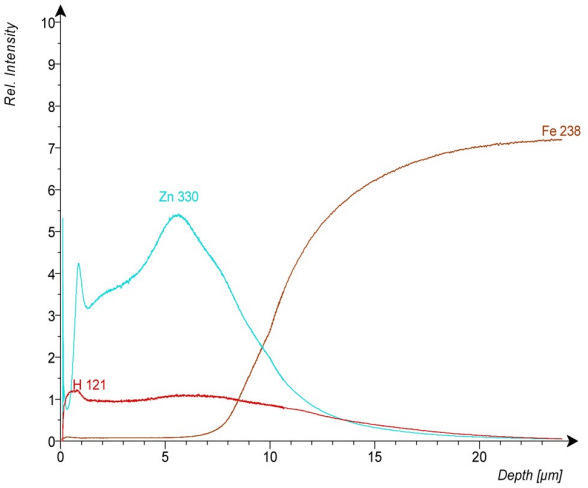

(a) Zinc plated bolt.

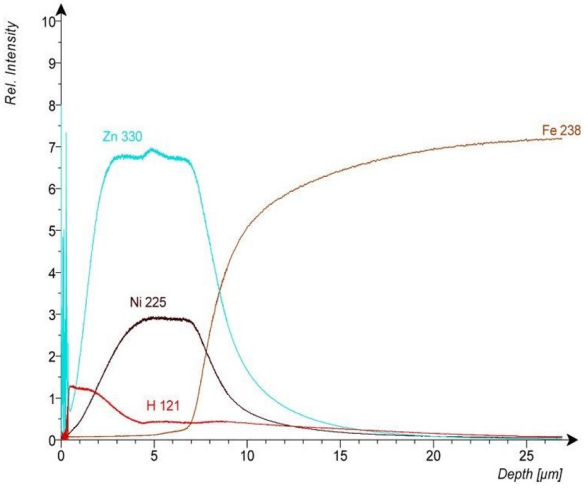

(b) Acidic zinc-nickel plated (ECOLUX STEEL^{TM}) bolt.

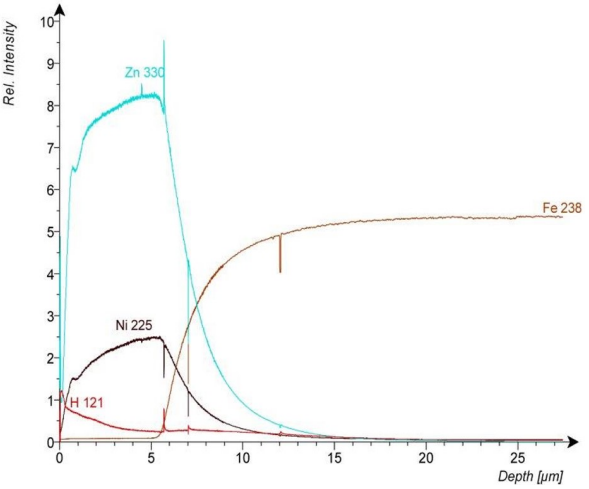

(c) Acidic zinc-nickel plated (ECOLUX STEEL^{TM}) and heat-treated bolt.

FIGURE 3.30: H, Zn, Ni and Fe GDOES depth profile of bolts with different plated layer: zinc, zinc nickel and heat-treated zinc nickel.

Chapter 4

Conclusions

We study commercial zinc nickel baths to plate 10 µm thick layer with a content of nickel from 12% to 16% working as corrosion resistance onto steel substrate. XRF, XRD, GDOES and SEM allow us to investigate additive effects on deposit composition, structure, morphology and phase. By means cyclic voltammetry we analyse electrochemical behaviour of solution varying additive content. We also consider some post-plating treatments, evaluating corrosion resistance by potentiodynamic polarization and phase change by diffraction.

ECOLUX STELL^{TM} assures easier plating and better layer. In the presence of additives, we can obtain optimal content of zinc and nickel with a wide range of deposition potential. Instead using acidic bath without additives nickel content increases with potential so only a narrow interval ensures good deposit.

Furthermore brightening agent provides flatter surface as we can see in SEM pictures: bath A sample presents compact layer with small crystals instead bath B sample is characterised by coarse structures with many cracks. Effect on aesthetical appearance is visible to the naked eye: samples A are brilliant with mirror effect; on the contrary, samples B are opaque.

Additives work synergistically, in particular ECOLUX STEEL A and ECOLUX STEEL C: if one of the two is absent, bath behaviour will get worse and ions will not be stable in solution.

Additives act their functions up to a certain value of deposition current, keeping nickel content in the optimal range. Beyond 100 mA/cm^2 organic compounds stop working so bath loses in repeatability and reproducibility.

Stirring has same effect with and without additives: continuous solution refresh near the cathode surface causes decrease of nickel content in favour of zinc and increase of growth rate for long time deposition.

As highlighted by GDOES analysis, acidic solutions assure homogeneous composition; in fact nickel and zinc depth profiles are almost constant. Additives reduce hydrogen content into the substrate near the interface, it has beneficial effect on steel because it decreases harmful hydrogen embrittlement. Fasteners analysis highlights this effect. Meanwhile zinc plated bolt has hydrogen species into substrate near the interface, ECOLUX STEEL^{TM} plating reduces hydrogen penetration and its content is very low into the substrate. After thermal treatment signal doesn't change, therefore zinc nickel plated bolt contains so little amount of hydrogen that dehydrogenization has almost no effect.

As XRD patterns show, acidic bath deposits contain mainly γ zinc nickel phase and grains are preferentially oriented along planes (330) and (411). Peaks of other phases (zinc, nickel and δ zinc nickel) are very low, only iron substrate is visible in all the samples. Therefore plated layer is monophasic γ, assuring best corrosion resistance.

XRD patterns show clearly additive effect: all diffraction γ peaks become much more intense indicating a more defined crystal structure and consequently a better behaviour against corrosion. Diffraction peaks of samples obtained with high deposition current are less intense; this means that additives can't work well in these condition.

Anodic peaks of cyclic voltammetries are interpreted with a double dissolution process of a the γ phase: dezincation at lower potential, then nickel oxidation due to its higher nobility.

ECOLUX STEEL A influences grain structure, in fact it modifies anodic branch of cyclic voltammetries; shifting of peak potential indicates that additive is adsorbed on surface. Instead with ECOLUX STEEL C currents of anodic peaks increases, indicating a greater amount of deposited phases.

Alkaline baths are slower due to lower current efficiency. In the absence of additives solution is unstable. Peaks in XRD pattern are the same found with acidic bath samples:

the deposit is almost all γ phase with preferential orientation along plane (330) (411). There are some traces of η phase. Crystal structure is less define than acidic sample, in fact peak intensity is lower.

Cyclic voltammetries confirms similarity with acidic bath: there are two anodic peaks indicating dissolution of zinc and nickel of γ phase. Additivo Ni b.d.c. doesn't influences clearly electrochemical bath behaviour.

Based on potentiodynamic polarization, passivation and heat treatment improve corrosion resistance of the coating. Presence of chromium reduces corrosion current, slowing degradation. After heat treatment nobility increases due to reorganization of zinc nickel γ phase; XRD pattern shows changes of crystal orientation: peak relatives to (442) (600) planes decreases, other peaks increases, in particular that relative to (330) (411) becomes the highest. This new crystal structure assures better behaviour against corrosion.

Bibliography

[1] Abou-Krisha, M. M., Assaf, F. H., & Toghan, A. A. (2007). Electrodeposition of Zn-Ni alloys from sulfate bath. *Journal of Solid State Electrochemistry*, *11*(2), 244–252.

[2] Abou-Krisha Ó ACA, M. M. (2012). Effect of pH and current density on the electrodeposition of Zn–Ni–Fe alloys from a sulfate bath.

[3] Albalat, R., Gómez, E., Müller, C., Pregonas, J., Sarret, M., & Vallés, E. (1991). Zinc-nickel coatings: Relationship between additives and deposit properties. *Journal of Applied Electrochemistry*, *21*(1), 44–49.

[4] Andrienko, D. (2008). Cyclic Voltammetry.

[5] Arezki, B. (2014). Advanced Physics Laboratory XRF X-Ray Fluorescence : Energy-Dispersive analysis (EDXRF). (pp. 1–14).

[6] Arsenault, B., Champagne, B., Lambert, P., & Dallaire, S. (1989). Zinc-nickel coatings for improved adherence and corrosion resistance. *Surface and Coatings Technology*, *37*(4), 369–378.

[7] Baldwin, K. R., Smith, C. J. E., & Robinson, M. J. (1994). A study into the electrodeposition mechanisms of zinc-nickel alloys from an acid-sulphate bath. *Transactions of the Institute of Metal Finishing*, *72*, 79–88.

[8] Baldwin, K. R., Smith, C. J. E., & Robinson, M. J. (1995). Cathodic protection of steel by electrodeposited zinc-nickel alloy coatings. *Corrosion*, *51*(12), 932–940.

[9] Barcelo, G., Garcia, E., Sarret, M., & Müller, C. (1998). Characterization of zinc-nickel alloys obtained from an industrial chloride bath. *Journal of Applied Electrochemistry*, *28*(28), 1113–1120.

[10] Brenner, A. (1963). Electrodeposition of Alloys. *vol.1, Aca*.

[11] Byk, T. V., Gaevskaya, T. V., & Tsybulskaya, L. S. (2008). Effect of electrodeposition conditions on the composition, microstructure, and corrosion resistance of Zn-Ni alloy coatings. *Surface and Coatings Technology*, *202*(24), 5817–5823.

[12] Cavallotti, P. L., Nobili, L., & Vicenzo, A. (2005). Phase structure of electrodeposited alloys. *Electrochimica Acta*.

[13] Chang, L. M., Chen, D., Liu, J. H., & Zhang, R. J. (2009). Effects of different plating modes on microstructure and corrosion resistance of Zn-Ni alloy coatings. *Journal of Alloys and Compounds*, *479*(1-2), 489–493.

[14] Conde, A., Arenas, M. A., & de Damborenea, J. J. (2011). Electrodeposition of Zn-Ni coatings as Cd replacement for corrosion protection of high strength steel. *Corrosion Science*, *53*(4), 1489–1497.

[15] Conrad, H. A., Corbett, J. R., & Golden, T. D. (2011). Electrochemical Deposition of γ-Phase Zinc-Nickel Alloys from Alkaline Solution.

[16] Conrad, H. A., McGuire, M. R., Zhou, T., Ibrahim Coskun, M., & Golden, T. D. (2015). Improved corrosion resistant properties of electrochemically deposited zinc-nickel alloys utilizing a borate electrolytic alkaline solution. *Surface and Coatings Technology*, *272*, 50–57.

[17] Darband, G. B., Afshar, A., & Aliabadi, A. (2015). Zn–Ni Electrophosphating on galvanized steel using cathodic and anodic electrochemical methods.

[18] DiBari, G. a. (2014). Nickel plating. *Metal Finishing*, *97*(1), 276–293.

[19] Dutra, C. a. M., Silva, J. W. J., & Nakazato, R. Z. (2013). Corrosion Resistance of Zn and Zn-Ni Electrodeposits : Morphological Characterization and Phases Identification. *2013*(October), 644–648.

[20] Ec (2000). DIRECTIVE 200053EC OF THE EUROPEAN PARLIAMENT AND OF THE COUNCIL on end-of life vehicles. *Official Journal of the European Communities*, *L 269*(September 2000), 1–15.

[21] El Hajjami, A., Gigandet, M. P., De Petris-Wery, M., Catonne, J. C., Duprat, J. J., Thiery, L., Raulin, F., Pommier, N., Starck, B., & Remy, P. (2007). Characterization of thin Zn-Ni alloy coatings electrodeposited on low carbon steel. *Applied Surface Science*, *254*(2), 480–489.

[22] Eliaz, N., Venkatakrishna, K., & Hegde, A. C. (2010). Electroplating and characterization of Zn-Ni, Zn-Co and Zn-Ni-Co alloys. *Surface and Coatings Technology*, *205*(7), 1969–1978.

[23] Fabri Miranda, F. J. (1999). Corrosion behavior of zinc-nickel alloy electrodeposited coatings. *Corrosion*, *55*(8), 732–742.

[24] Fashu, S., Gu, C. D., Wang, X. L., & Tu, J. P. (2014). Influence of electrodeposition conditions on the microstructure and corrosion resistance of Zn-Ni alloy coatings from a deep eutectic solvent. *Surface and Coatings Technology*, *242*, 34–41.

[25] Fei, J. Y., & Wilcox, G. D. (2006). Electrodeposition of zinc-nickel compositionally modulated multilayer coatings and their corrosion behaviours. *Surface and Coatings Technology*, *200*(11), 3533–3539.

[26] Feng, Z., Li, Q., Zhang, J., Yang, P., & An, M. (2015). Electrochemical Behaviors and Properties of Zn-Ni Alloys Obtained from Alkaline Non-Cyanide Bath Using 5,5'-Dimethylhydantoin as Complexing Agent. *Journal of the Electrochemical Society*, *162*(9), D412–D422.

[27] Feng, Z., Li, Q., Zhang, J., Yang, P., Song, H., & An, M. (2015). Electrodeposition of nanocrystalline Zn-Ni coatings with single gamma phase from an alkaline bath. *Surface and Coatings Technology*.

[28] Fratesi, R., & Roventi, G. (1992). Electrodeposition of zinc-nickel alloy coatings from a chloride bath containing NH4Cl. *Journal of Applied Electrochemistry*, *22*(7), 657–662.

[29] Fratesi, R., & Roventi, G. (1996). Corrosion resistance of Zn-Ni alloy coatings in industrial production. *Surface and Coatings Technology*, *82*(1-2), 158–164.

[30] Galleani, S., & Spina, U. (2013). ECOLUX STEEL Scheda tecnica. (Mi), 1–6.

[31] Galvanizers Association (2012). The Basics of Hot Dip Galvanized Steel. (pp. 1–25).

[32] Gavrila, M., Millet, J. P., Mazille, H., Marchandise, D., & Cuntz, J. M. (2000). Corrosion behaviour of zinc-nickel coatings, electrodeposited on steel. *Surface and Coatings Technology*, *123*(2-3), 164–172.

[33] Gou, S. P., & Sun, I. W. (2008). Electrodeposition behavior of nickel and nickel-zinc alloys from the zinc chloride-1-ethyl-3-methylimidazolium chloride low temperature molten salt. *Electrochimica Acta*, *53*(5), 2538–2544.

[34] Higashi, K., Hayashi, Y., Fukushima, H., Akiyama, T., & Hagi, H. (2009). A fundamental study of corrosion-resistant zinc-nickel electroplating. (pp. 1–30).

[35] Hosseini, M. G., Ashassi-Sorkhabi, H., & Ghiasvand, H. A. Y. (2008). Electrochemical studies of Zn-Ni alloy coatings from non-cyanide alkaline bath containing tartrate as complexing agent. *Surface and Coatings Technology*, *202*(13), 2897–2904.

[36] Iacoviello, F., & Di Cocco, V. (2014). Analisi metallografica di leghe ferrose e non ferrose. (Uni 3138), 126–147.

[37] Johansson, A., Ljung, H., & Westman, S. (1968). X-Ray and Neutron Diffraction Studies on ZnNi and ZnFe.

[38] Kim, H., Popov, B. N., & Chen, K. S. (2003). Comparison of corrosion-resistance and hydrogen permeation properties of Zn-Ni, Zn-Ni-Cd and Cd coatings on low-carbon steel. *Corrosion Science*, *45*(7), 1505–1521.

[39] Kwon, M., hwan Jo, D., Cho, S. H., Kim, H. T., Park, J. T., & Park, J. M. (2016). Characterization of the influence of Ni content on the corrosion resistance of electrodeposited Zn-Ni alloy coatings. *Surface and Coatings Technology*, *288*, 163–170.

[40] Lee, H. Y., & Kim, S. G. (2000). Characteristics of Ni deposition in an alkaline bath for Zn-Ni alloy deposition on steel plates. *Surface and Coatings Technology*, *135*(1), 69–74.

[41] Lehmberg, C. E., Lewis, D. B., & Marshall, G. W. (2005). Composition and structure of thin electrodeposited zinc-nickel coatings. *Surface and Coatings Technology*, *192*(2-3), 269–277.

[42] Li, G. Y., Lian, J. S., Niu, L. Y., & Jiang, Z. H. (2005). Investigation of nanocrystalline zinc-nickel alloy coatings in an alkaline zincate bath. *Surface and Coatings Technology*, *191*(1), 59–67.

[43] Lou, H. H., & Huang, Y. (1978). Electroplating. *Encyclopedia of chemical processing*, *1*, 839–848.

[44] Magagnin, L., Nobili, L., & Cavallotti, P. L. (2015). Metastable zinc-nickel alloys deposited from an alkaline electrolyte. *Journal of Alloys and Compounds*, *615*(S1), S663–S666.

[45] Mathias, M. F., Villa, C. M., & Chapman, T. W. (1990). A model of zinc-nickel alloy electrodeposition in an industrial-scale cell. *Journal of Applied Electrochemistry*, *20*(1), 1–10.

[46] Muller, C., Sarret, M., & Benballa, M. (2002). Complexing agents for a Zn – Ni alkaline bath. *Journal of Electroanalytical Chemistry*, *519*, 85 – 92.

[47] Muresan, L. M., Eymard, J., Blejan, D., & Indrea, E. (2010). Zn-Ni alloy coatings from alkaline bath containing triethanolamine. influence of additives. *Studia Universitatis Babes-Bolyai Chemia*, *1*, 37–43.

[48] Ohtsuka, T., & Komori, A. (1998). Study of initial layer formation of Zn-Ni alloy electrodeposition by in situ ellipsometry. *Electrochimica Acta*, *43*(21-22), 3269–3276.

[49] Oriti, T. (2014). A Comparative Study of Gamma-Phase Zinc-Nickel Deposits Electroplated from Various Alkaline and Acid Systems. *NASF SURFACE TECHNOLOGY WHITE PAPERS*, *79*(1), 1–16.

[50] Osborne, K. (2005). Electoplating. *VIII-Metals-G-Electroplating*, (pp. 1–8).

[51] Pedroza, G. A. G., de Souza, C. A. C., de Jesus, M. D., de Andrade Lima, L. R. P., & Ribeiro, D. V. (2014). Influence of formic acid on the microstructure and corrosion resistance of Zn-Ni alloy coatings by electrodeposition. *Surface and Coatings Technology*, *258*, 232–239.

[52] Protti, P. (2001). Introduzione alle moderne tecniche di Analisi Voltammetriche e Polarografiche.

[53] Rizwan, R., Mehmood, M., Imran, M., Ahmad, J., Aslam, M., & Akhter, J. I. (2007). Deposition of Nanocrystalline Zinc-Nickel Alloys by D.C. Plating in Additive Free Chloride Bath. *Materials Transactions*, *48*(6), 1558–1565.

[54] Rodriguez-Torres, I., Valentin, G., & Lapicque, F. (1999). Electrodeposition of zinc-nickel alloys from ammonia-containing baths. *Journal of Applied Electrochemistry*, *29*(9), 1035–1044.

[55] Roventi, G. (2015). Electrodeposition of Nickel-Zinc Alloy from a Sulfamate Bath. *4*, 21–26.

[56] Schlesinger, M., Paunovic, M., & Snyder, D. D. (2010). Cap 1, Fundamental considerations. *Modern Electroplating (5th edition)*, (pp. 1–32).

[57] Shoeib, M. A. (2011). Electrodeposited zinc/nickel coatings- A review.

[58] Singleton, R. (1994). BARREL PLATING.

[59] Sohi, M. H., & Jalali, M. (2003). Study of the corrosion properties of zinc-nickel alloy electrodeposits before and after chromating. *Journal of Materials Processing Technology*, *138*(1-3), 63–66.

[60] Tian, W., Xie, F. Q., Wu, X. Q., & Yang, Z. Z. (2009). Study on corrosion resistance of electroplating zinc-nickel alloy coatings. *Surface and Interface Analysis*, *41*(3), 251–254.

[61] Tsybulskaya, L., Gaevskaya, T., Purovskaya, O., & Byk, T. (2008). Electrochemical deposition of zinc–nickel alloy coatings in a polyligand alkaline bath. *Surface and Coatings Technology*, *203*(3-4), 234–239.

[62] Winand, R. (2011). Cap 10, Electrodeposition of Zinc and Zinc Alloys. *Modern Electroplating: Fifth Edition*, (pp. 285–307).

[63] Wu, Z., Fedrizzi, L., & Bonora, P. L. (1996). Electrochemical studies of zinc-nickel codeposition in chloride baths. *Surface and Coatings Technology*, *85*, 170–174.

[64] Xiong, W., Xu, H., & Du, Y. (2011). Thermodynamic investigation of the galvanizing systems, II: Thermodynamic evaluation of the NiZn system. *Calphad: Computer Coupling of Phase Diagrams and Thermochemistry*.

[65] Zaky, A. M., Assaf, F. H., & Ali, F. E. Z. a. H. (2011). Electrochemical Behavior of Zn-Ni Alloys in Borate Buffer Solutions. *ISRN Materials Science*.